Advanced Workshop on Earthquake Fault Mechanics: Theory, Simulation and Observations

ICTP, Trieste, Sept 2-14 2019

Lecture 7: finite source inversion

Jean Paul Ampuero (IRD/UCA Geoazur)

Finite source inversion

- Definition of the inverse problem
- Data and fundamental limitations
- G analysis in toy model
- G analysis in real situations and SIV benchmark
- Regularization
- Bayesian inversion
- Joint inversion of multiple data
- Uncertainty quantification and visualization
- Model errors Cp (velocity model, fault geometry)

Detailed source parameters

Outputs of dynamic rupture models:

Detailed space-time distribution of slip on the fault

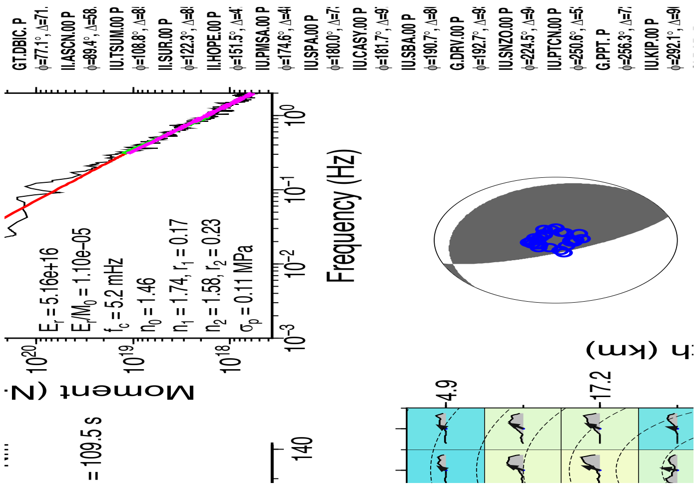

+ seismograms & ground displacements

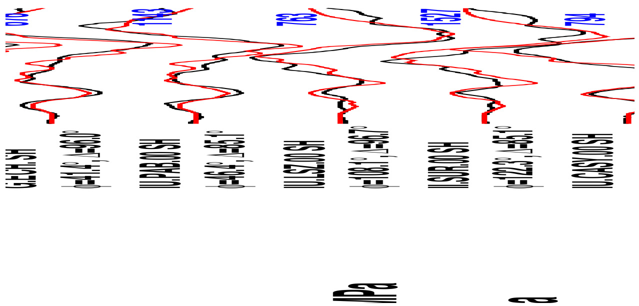

From ground motion recordings …

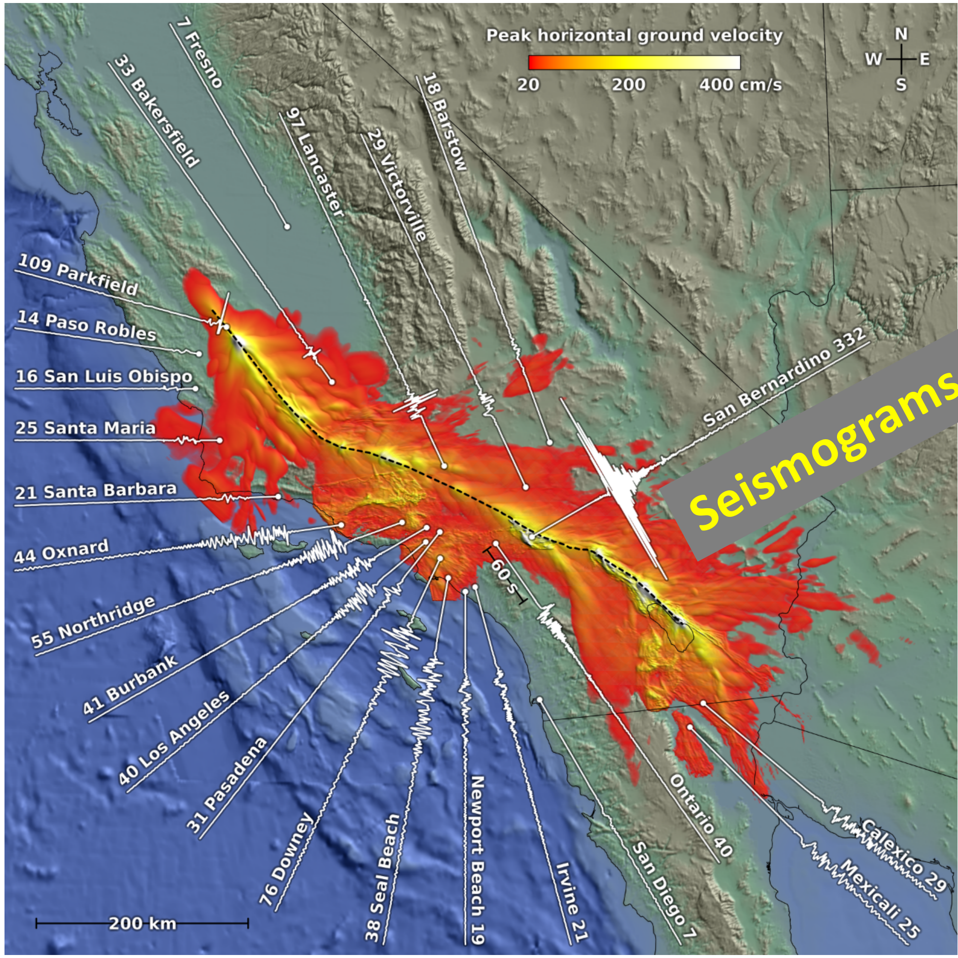

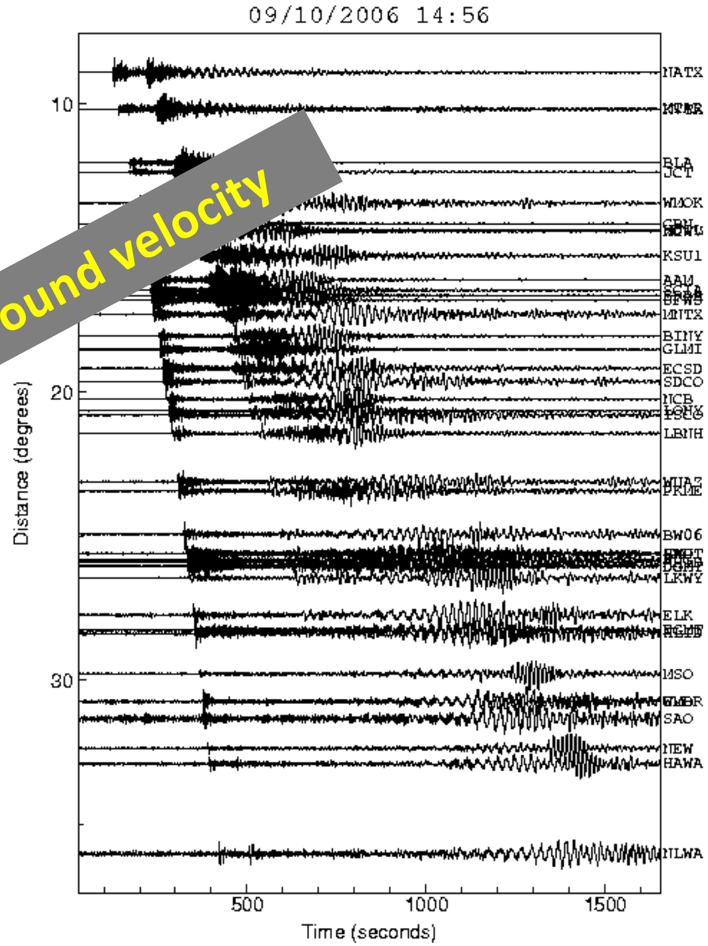

From ground motion recordings to the rupture process

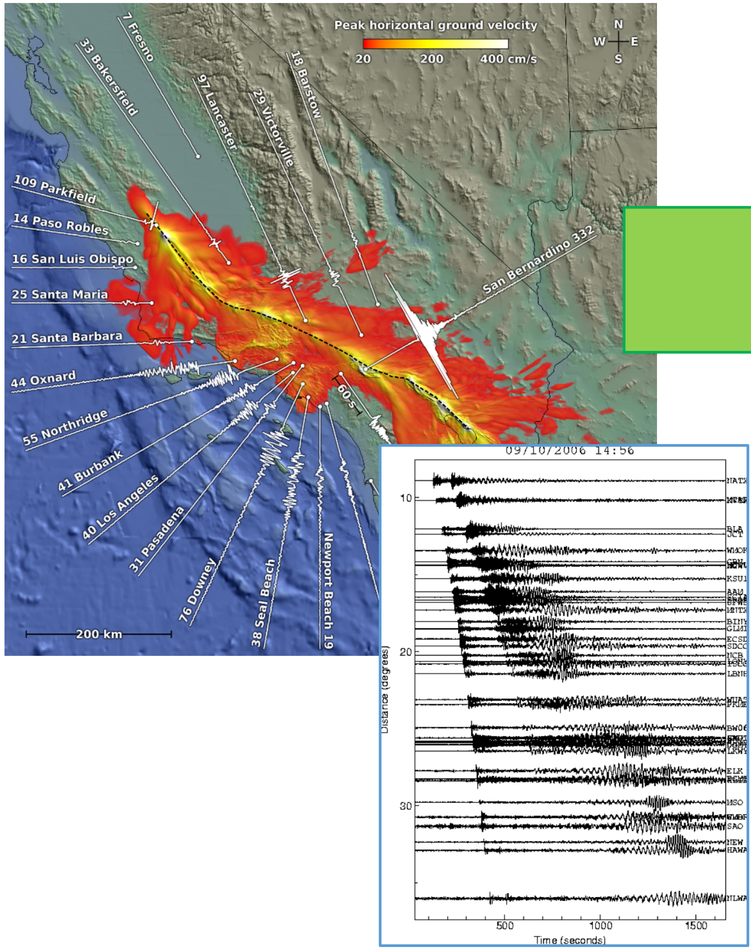

How much did the **fault** slip?

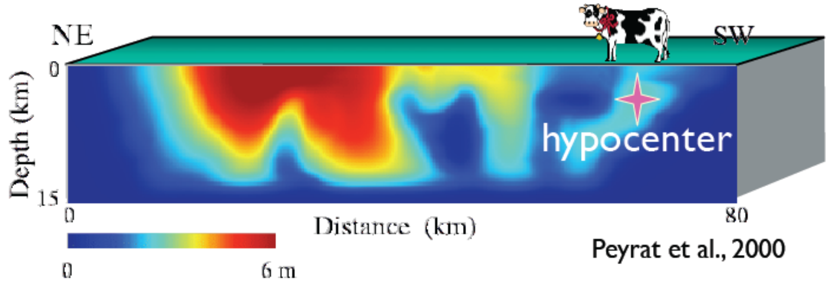

How did it slip?

Fast/slow? Smooth/tortuous? Loud/silent?

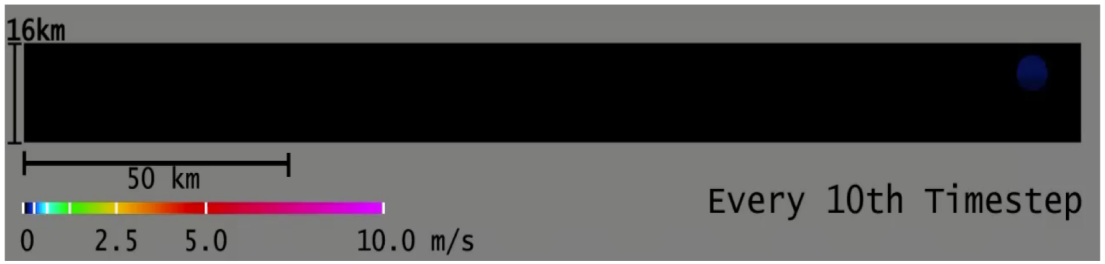

Finite source seismograms

Representation theorem:
seismogram = sum of (Green's function)*(slip rate)
over the whole fault

$$d_i(r,t) = \iint_{fault} G_{ij}(x,r,t) * \dot{D}_j(x,t)\, dx^2$$

* means convolution
G can be a synthetic or empirical Green's function

$$d = G \cdot m$$

data ←→ model

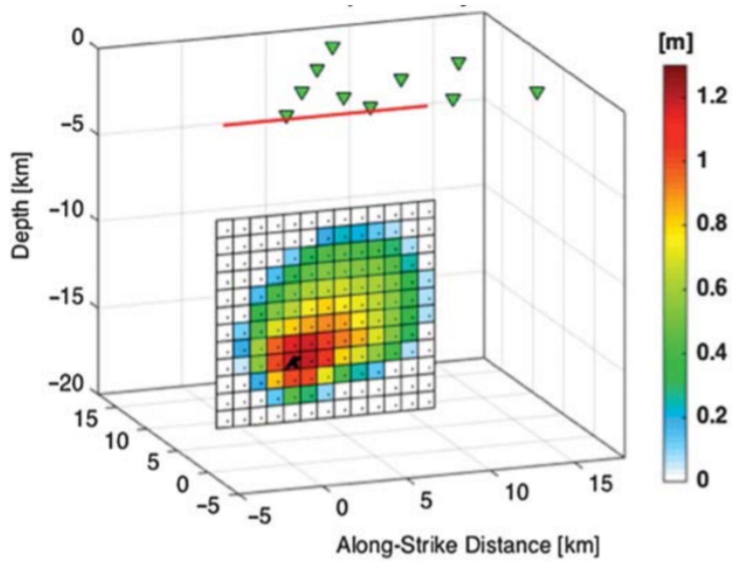

Linear and non-linear parameterizations

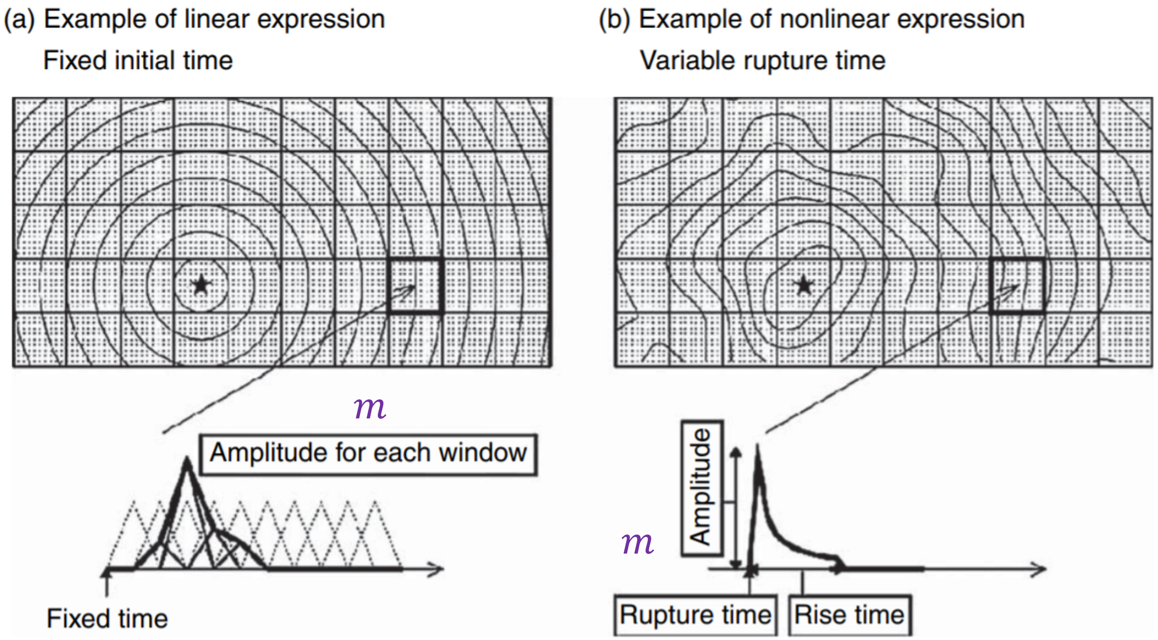

$$d = G \cdot m$$

$$d = G(m)$$

Linear inversion

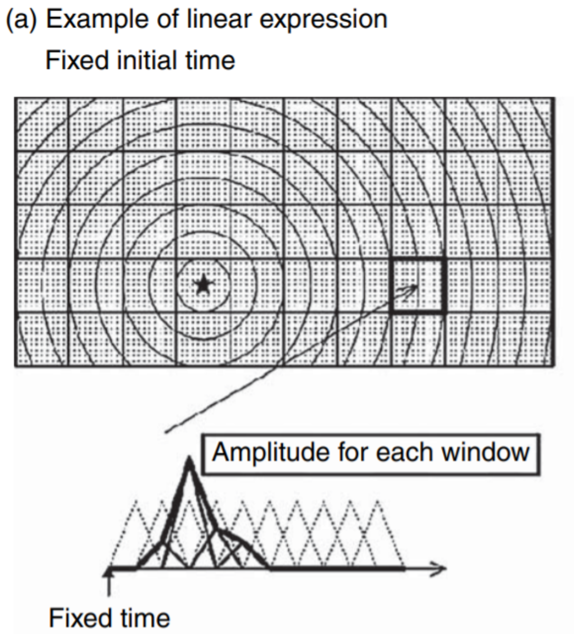

$$d = G \cdot m$$

Structure of the G matrix …

Linear inversion

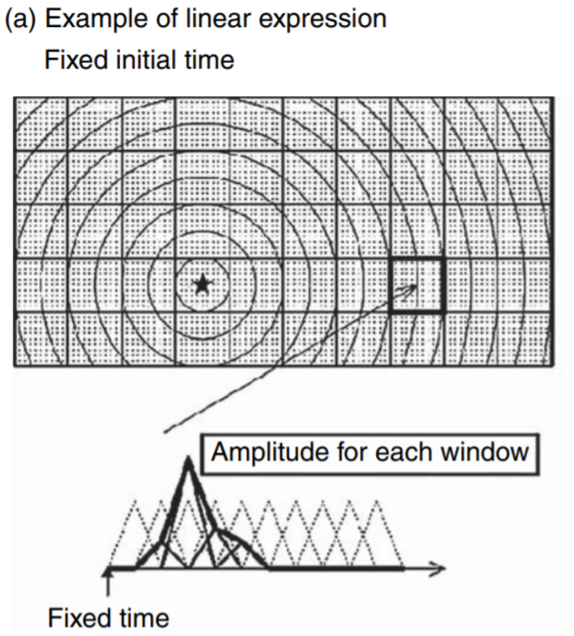

Find m^* that minimizes the cost function

$$C(m) = \|d - G \cdot m\|^2$$

Least-squares solution

$$m^* = (G^T G)^{-1} G^T d$$

Including data covariance matrix C_d :

$$C(m) = (d - G \cdot m)^T C_d^{-1} (d - G \cdot m)$$

Least-squares solution

$$m^* = \left(G^T C_d^{-1} G\right)^{-1} G^T d$$

Uncertainty quantified by model covariance: $C_m = \left(G^T C_d^{-1} G\right)^{-1}$

Limitations

Resolution (ambiguity at small scales)
Frequency band of Green's functions is limited
Frequency band of data is limited (attenuation, noise, instrument sensitivity)
Coverage of the wavefield is incomplete
Fault geometry is uncertain
…

Local, regional, teleseismic waves

Three characteristic ranges used in seismic studies:

0°-13° near-field or regional range: crustal phases, spherical geometry can be neglected

13°-30° upper-mantle distance range. Dominated by upper mantle triplications.

30°-180° teleseismic range: waves that sample lower mantle, core, upper mantle reverberations.

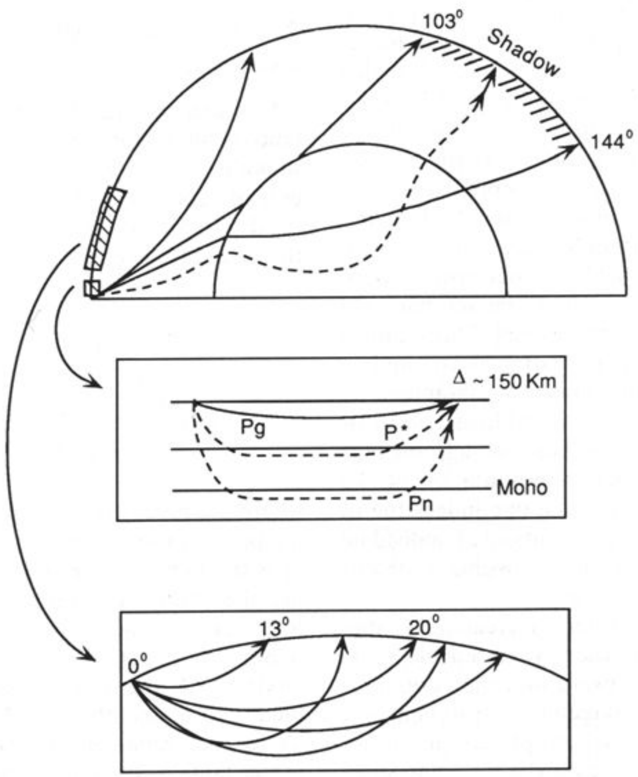

Fundamental limitations of teleseismic data

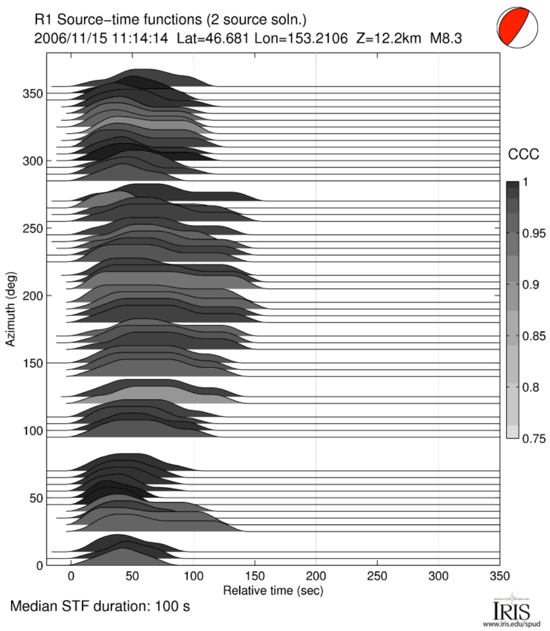

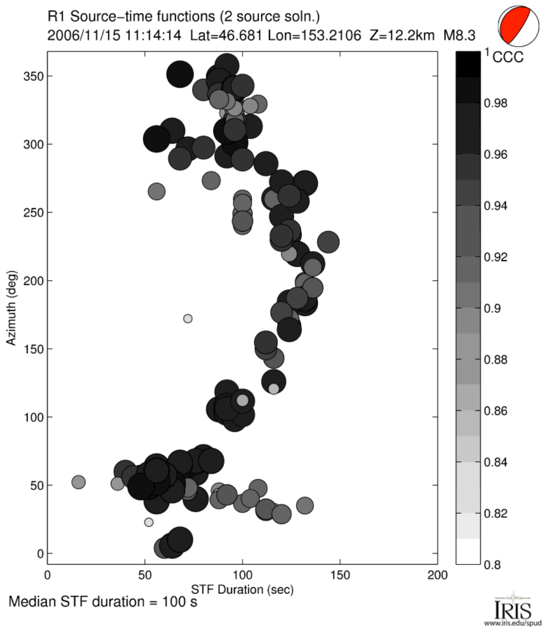

Apparent Source Time Function (Fraunhofer approximation) at a station located at direction $\hat{\boldsymbol{r}}_{\mathbf{0}}$ from the source:

$$\Omega(\hat{\boldsymbol{r}}_{\mathbf{0}},\tau)=\iint_{\Sigma}\dot{D}\left(\boldsymbol{\xi},\tau+\frac{\boldsymbol{\xi}\cdot\hat{\boldsymbol{r}}_0}{c}\right)d^2\xi$$

Fundamental limitations of teleseismic data

Fourier transform of Apparent Source Time Function:

$$\Omega(\hat{\boldsymbol{r}}_{\boldsymbol{0}}, \omega) = \iint_{\Sigma} \dot{D}(\boldsymbol{\xi}, \omega) \exp\left(-\mathrm{i}\omega \frac{\boldsymbol{\xi} \cdot \hat{\boldsymbol{r}}_0}{c}\right) d^2\xi$$

Spatial Fourier transform of a function $f(\boldsymbol{\xi})$ defined on the fault surface ($\boldsymbol{\xi} \in \Sigma$):

$$f(\boldsymbol{k}) = \iint_{\Sigma} f(\boldsymbol{\xi}) \exp(-\mathrm{i}\, \boldsymbol{\xi} \cdot \boldsymbol{k})\, d^2\xi$$

where $\boldsymbol{k}$ is a wavenumber vector along the fault.

→ ASTF is related to the spatial Fourier transform of slip rate by

$$\Omega(\hat{\boldsymbol{r}}_{\boldsymbol{0}}, \omega) = \dot{D}\left(\boldsymbol{k} = \frac{\omega \hat{\boldsymbol{\gamma}}_0}{c}, \omega\right)$$

where $\hat{\boldsymbol{\gamma}}_0 = \hat{\boldsymbol{r}}_0 - (\hat{\boldsymbol{r}}_0 \cdot \boldsymbol{n})\boldsymbol{n}$ = projection of $\hat{\boldsymbol{r}}_0$ on the fault surface Σ.

Fundamental limitations of teleseismic data

ASTF is related to the spatial Fourier transform of slip rate by

$$\Omega(\hat{\boldsymbol{r}}_{\boldsymbol{0}}, \omega) = \dot{D}\left(\boldsymbol{k} = \frac{\omega \widehat{\boldsymbol{\gamma}}_0}{c}, \omega\right)$$

where $\widehat{\boldsymbol{\gamma}}_0 = \hat{\boldsymbol{r}}_0 - (\hat{\boldsymbol{r}}_0 \cdot \boldsymbol{n})\boldsymbol{n} =$ projection of $\hat{\boldsymbol{r}}_0$ on the fault surface Σ.

If we measure $\dot{D}(\boldsymbol{k}, \omega)$ for all $\boldsymbol{k}$ and ω, we can infer $\dot{D}(\boldsymbol{\xi}, t)$ by inverse Fourier transform.

But the sampling is limited to $|\widehat{\boldsymbol{\gamma}}_0| < 1$

→ far-field source inversion is limited to fault wavenumbers such that $|\omega/k| > c$

(along-fault phase velocity higher than wave speed),

fault wavelengths $\lambda > c/f$.

(Source components with $|\omega/k| < c$ are associated to evanescent waves with exponential decay in the fault-normal direction, which do not make it to far field distances.)

To extract finer information about source processes, near-field ground motion recordings are needed.

3 source inversion models of the 1999 Chi-Chi earthquake

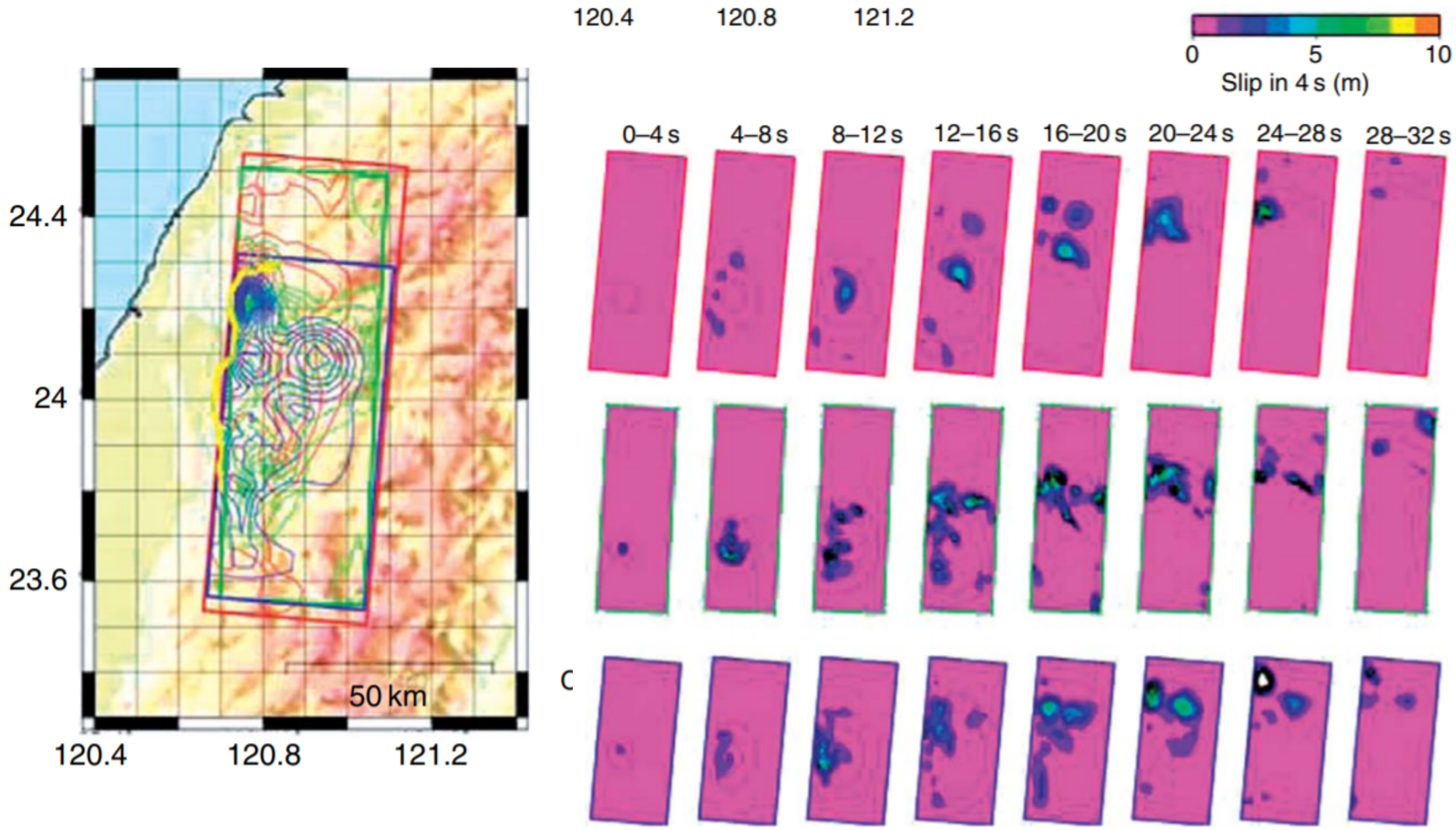

Ide (2015)

4 source inversion models of the 1999 Mw 7.6 Izmit earthquake

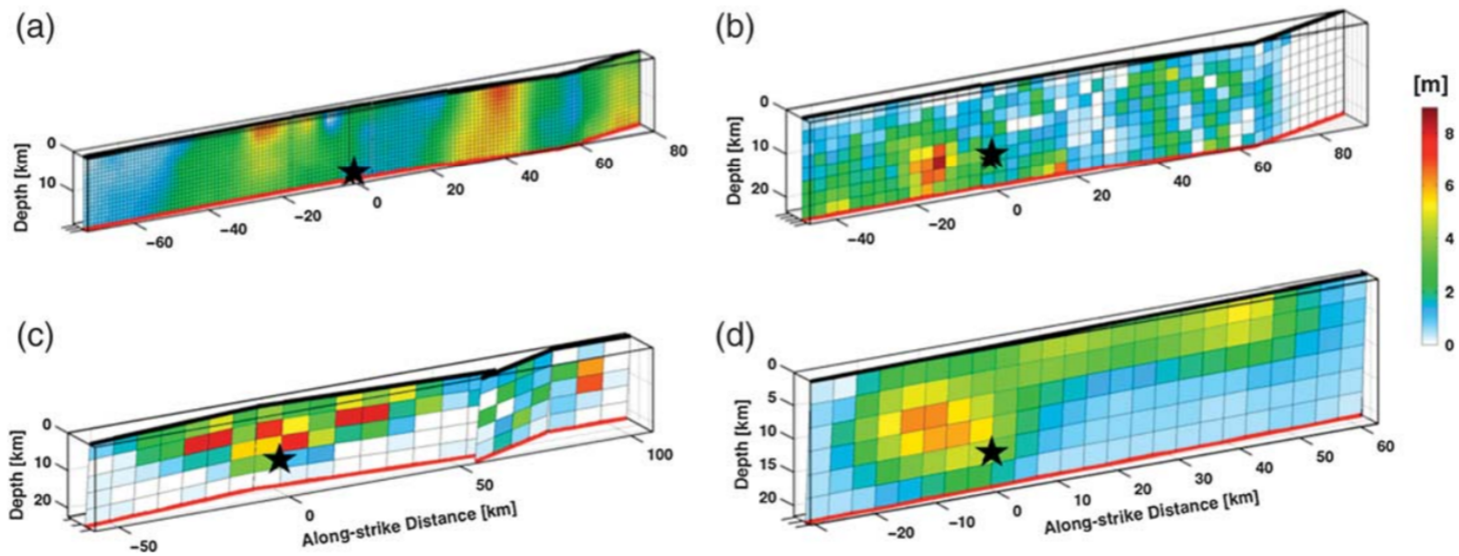

Mai et al (SRL 2016)

Potential sources of discrepancy:

- data selection and processing;
- methods used for computing the Green's functions
- the assumed Earth structure, fault geometry, etc
- method and parameterization for the inversion itself (linearized or fully nonlinear inversion; spatial and temporal discretization; applied smoothing and regularization)

What do we need to learn about earthquakes?

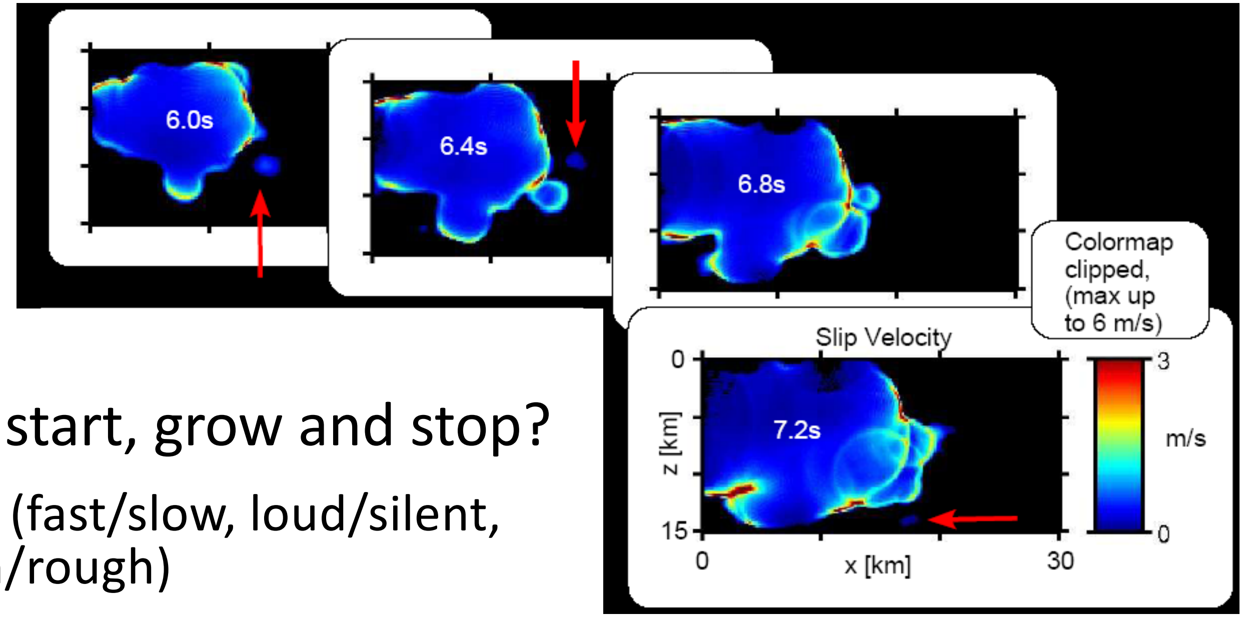

Why do earthquakes start, grow and stop?

How do faults slip? (fast/slow, loud/silent, smooth/rough)

We need to **image** the rupture process with **high definition**

Observational challenges

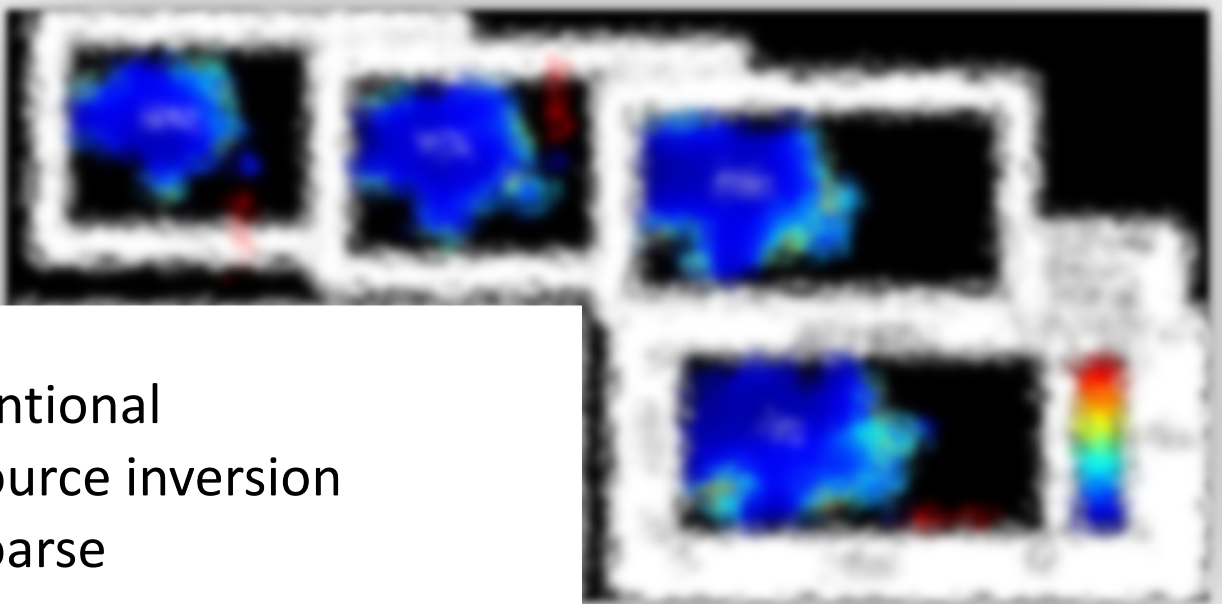

Conventional
earthquake source inversion
is coarse

We need to **image** the rupture process with **high definition**

Singular Value Decomposition of the inverse problem

Inverse problem: find m such that $d \approx G \cdot m$

SVD: $G = U \Lambda V^T$ where Λ is a diagonal matrix containing the eigenvalues λ_i of $G^T G$

- The generalized solution of the inverse problem, $m = G^{\#} d$, can be expressed as a linear combination of singular vectors $V_{(i)}$:

$$m = \sum_{i=1}^{M} \widetilde{m}_i V_{(i)} \quad \text{where} \quad \widetilde{m}_i = U_{(i)} \cdot d/\lambda_i$$

- The data vector can be expressed as

$$d = \sum_{i=1}^{N} \tilde{d}_i U_{(i)} \quad \text{where} \quad \tilde{d}_i = U_{(i)} \cdot d$$

→ the spectral components of data and model are related by

$$\widetilde{m}_i = \tilde{d}_i/\lambda_i$$

Singular Value Decomposition of the inverse problem

Inverse problem: find m such that $d \approx G \cdot m$
Eigenvalues λ_i of $G^T G$

→ the spectral components of data and model are related by

$$\tilde{m}_i = \tilde{d}_i / \lambda_i$$

- → the smaller is the singular value λ_i, the less sensitive is the data component to a given change of the corresponding model component
- → the singular value bears information about the sensitivity of the data to the particular basis function in the model space.
- → if λ_i is small, errors in the data or in the G matrix get amplified.
- → the components of the data associated to small eigenvalues are hardly recoverable by the inverse problem, they define an effective **null space**.

Lessons from a toy model

Toy model, Simple case 1 :

- Monochromatic vertical line source, frequency ω_0
- Acoustic medium (infinite, homogeneous)

Goal : given ground motions $d(x)$, recover source amplitude $m(z)$

$d = Gm$

$$d(x,\omega_0) = \int_{z_1}^{z_2} G(x,\omega_0,z)\cdot m(z)\cdot dz$$

Green's function

$$G(x,\omega_0,z) = \frac{\exp\left(-i\omega_0\sqrt{x^2+z^2}/c\right)}{4\pi\sqrt{x^2+z^2}}$$

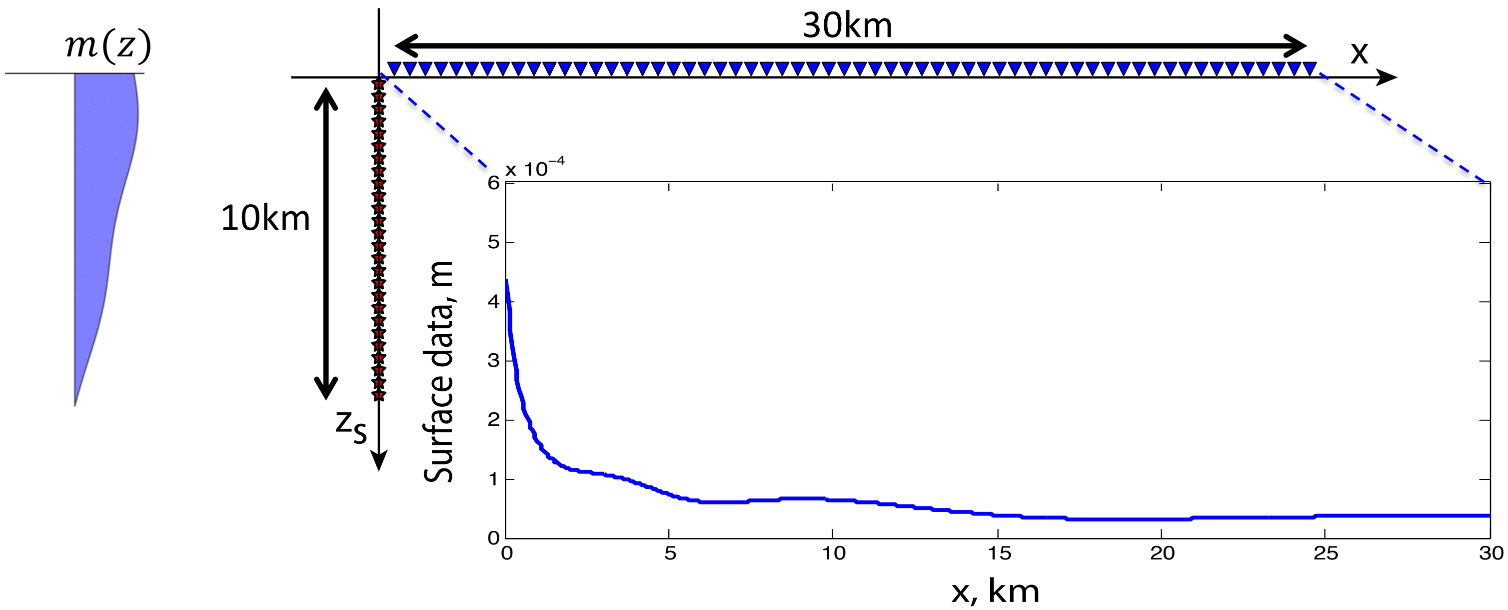

Seismic tremor in a glacier moulin

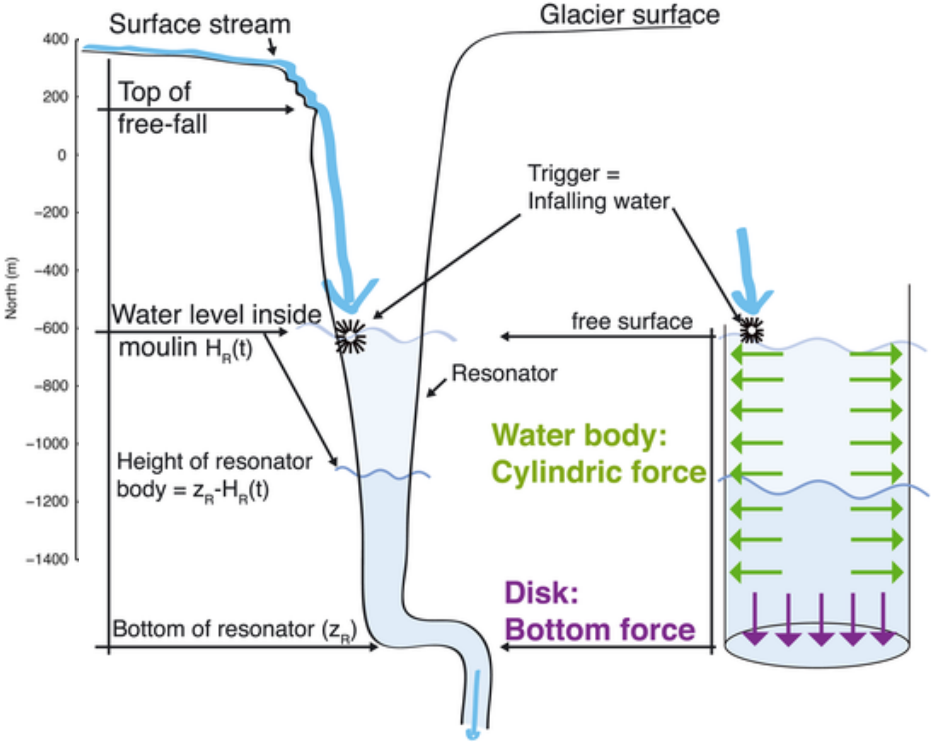

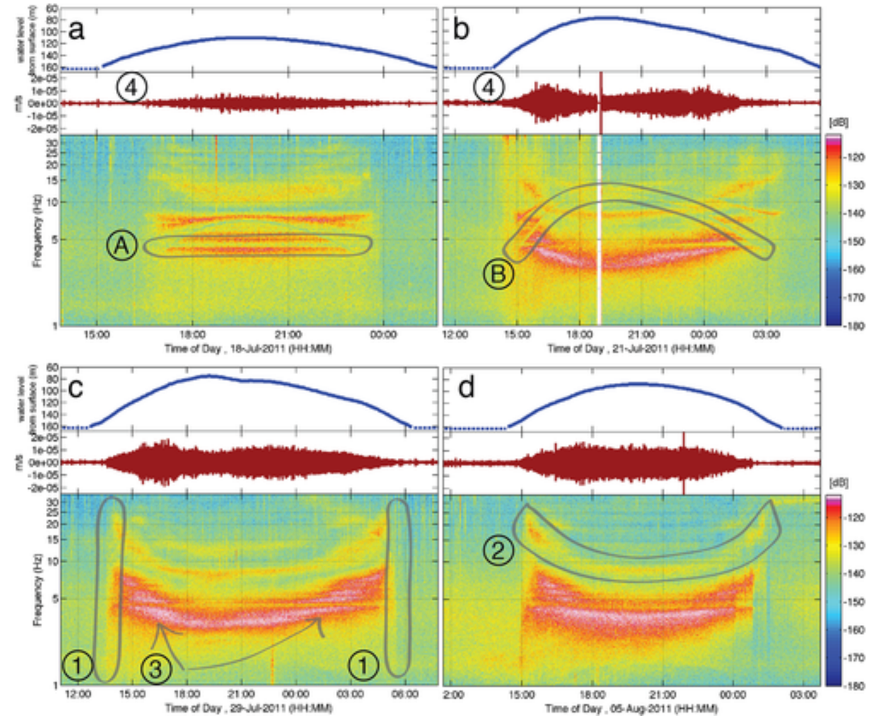

<u>Toy model, Simple case 1</u> :

- Monochromatic vertical line source,
- Acoustic medium (infinite, homogeneous)

Results for f_0=1Hz

$$d = G \cdot m$$

$$m = (G^T \cdot G)^{-1} \cdot G^T \cdot d$$

Condition Number !!!

v=4.2e+15

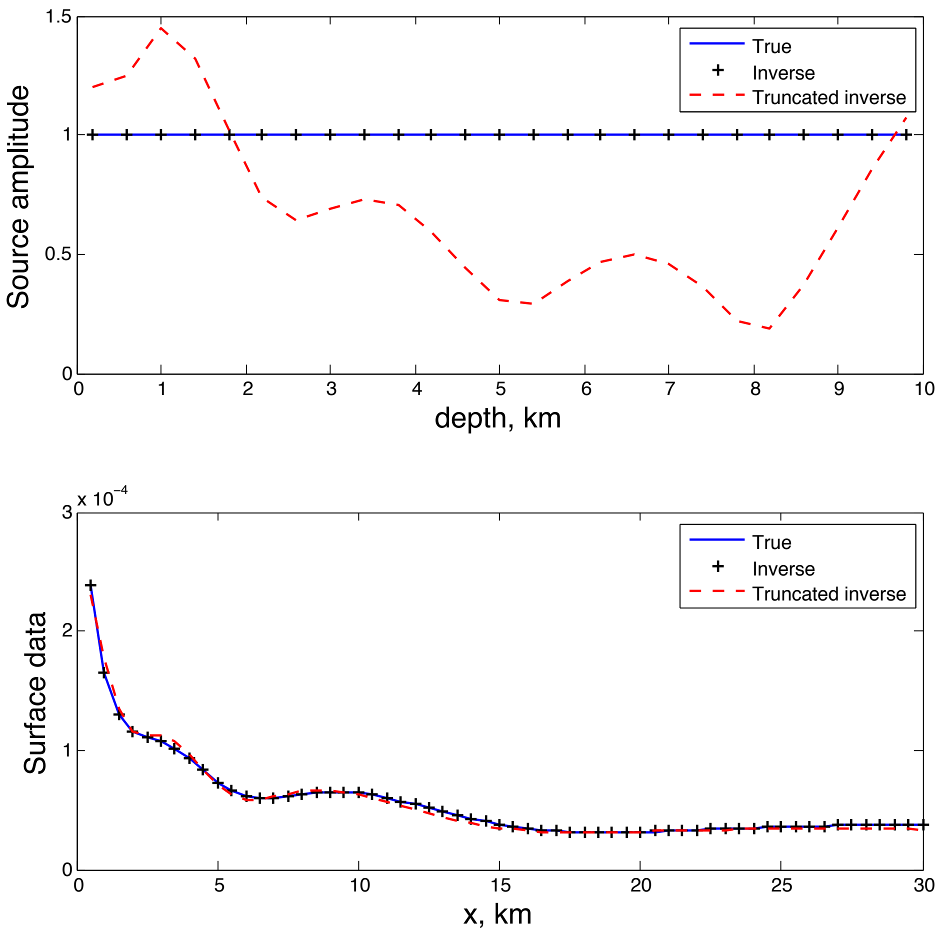

Toy model, Simple case 1 :

- Monochromatic vertical line source,
- Acoustic medium (infinite, homogeneous)

EIGENVALUES, EIGENVECTORS

Results for f_0=1Hz

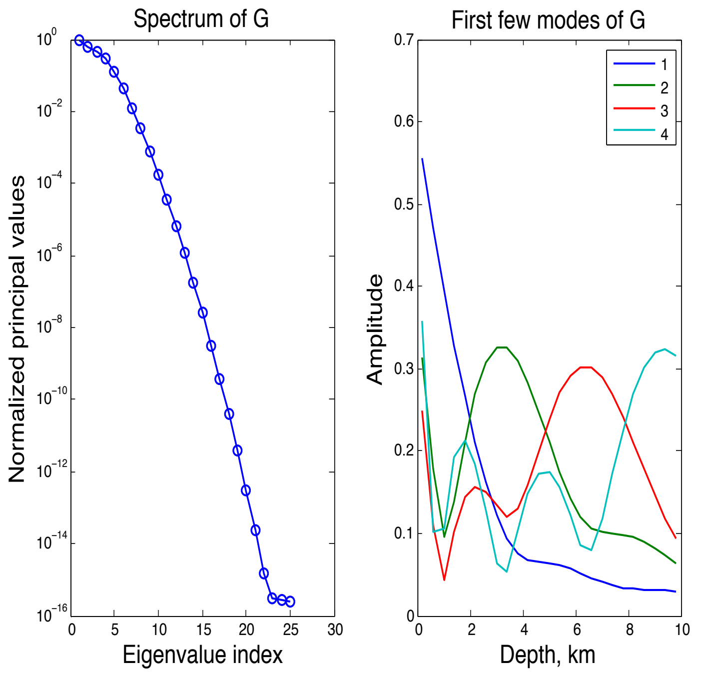

Results for f_0=10Hz

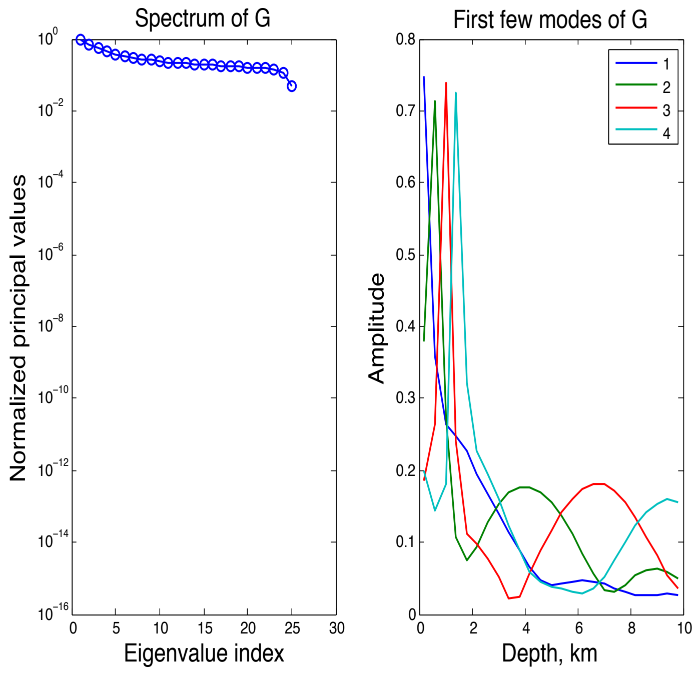

Toy model, Simple case 1 :

- Monochromatic vertical line source,
- Acoustic medium (infinite, homogeneous)

RESOLUTION MATRICES

Results for f_0=1Hz

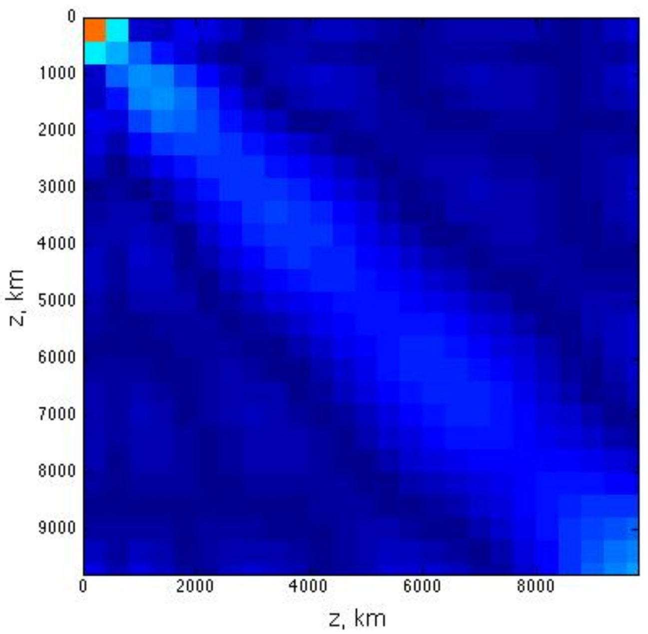

Results for f_0=10Hz

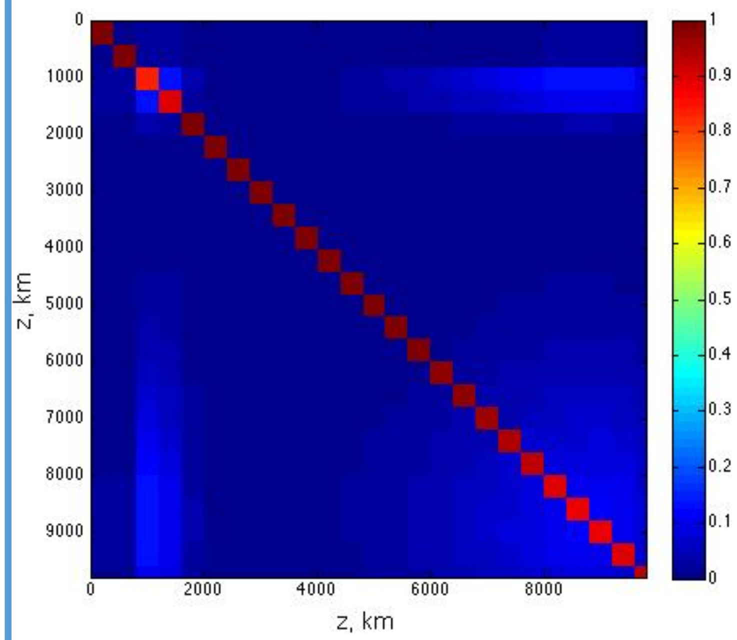

Toy model, Simple case 1 :

- Monochromatic vertical line source,
- Acoustic medium (infinite, homogeneous)

INVERSION RESULTS

Results for f_0=1Hz

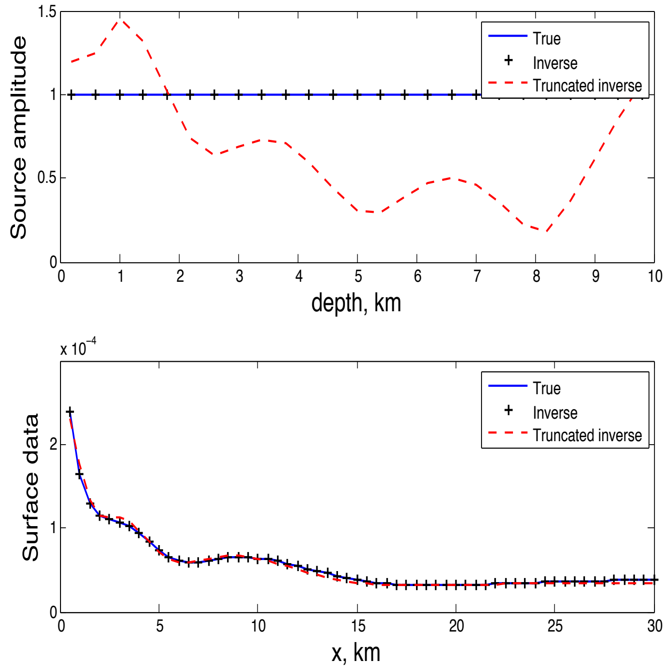

Results for f_0=10Hz

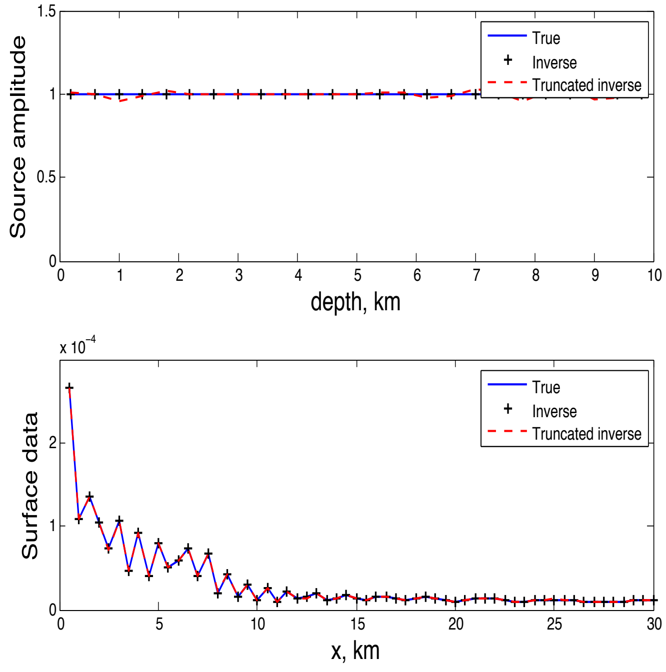

The anatomy of a
real earthquake source inversion problem

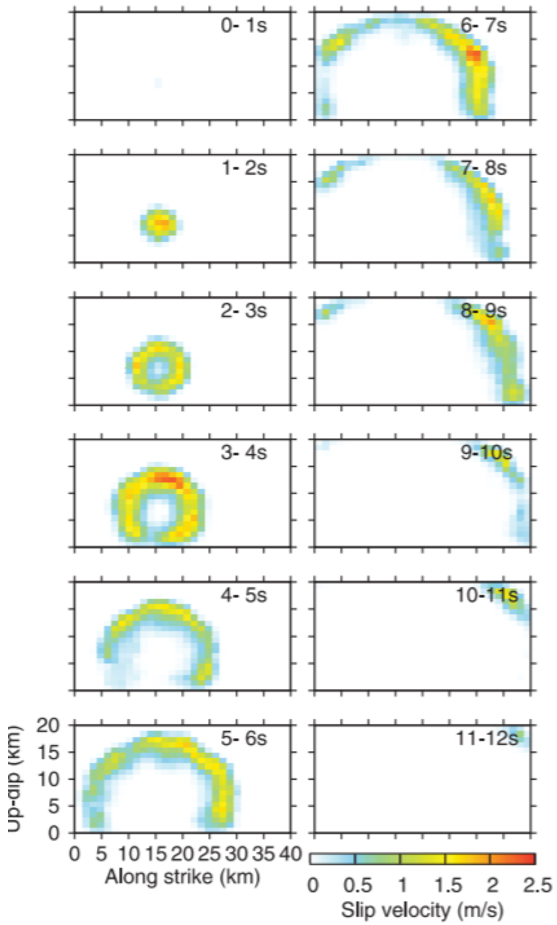
0- 1s
1- 2s
2- 3s
3- 4s
4- 5s
5- 6s
6- 7s
7- 8s
8- 9s
9-10s
10-11s
11-12s
Up-dip (km)
Along strike (km)
Slip velocity (m/s)

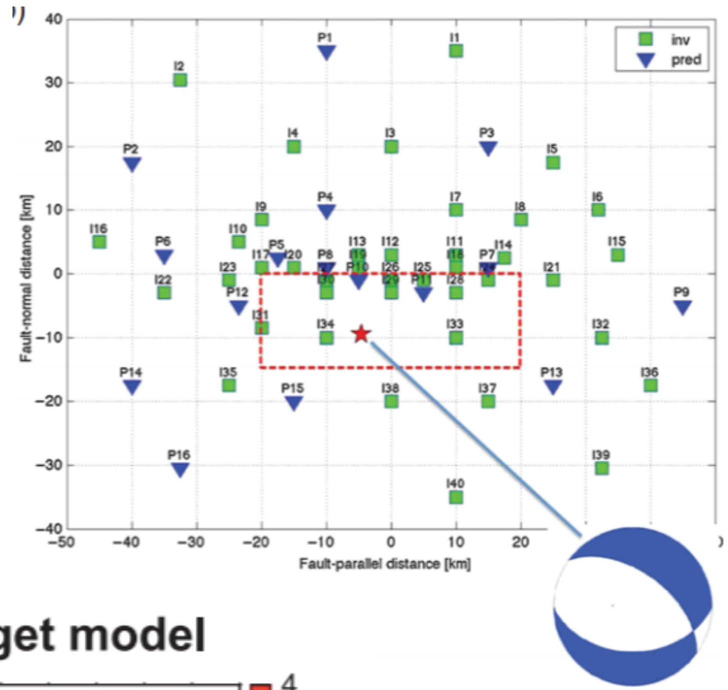
inv
pred
Fault-normal distance [km]
Fault-parallel distance [km]

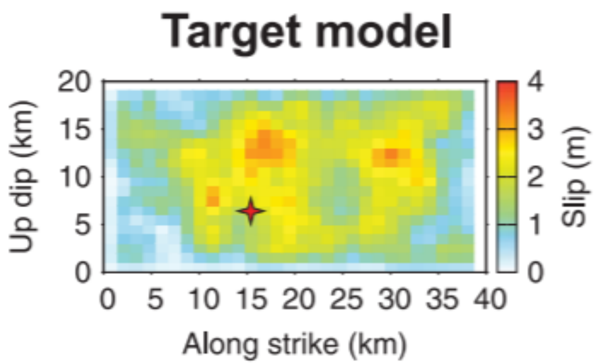
Target model
Up dip (km)
Along strike (km)
Slip (m)

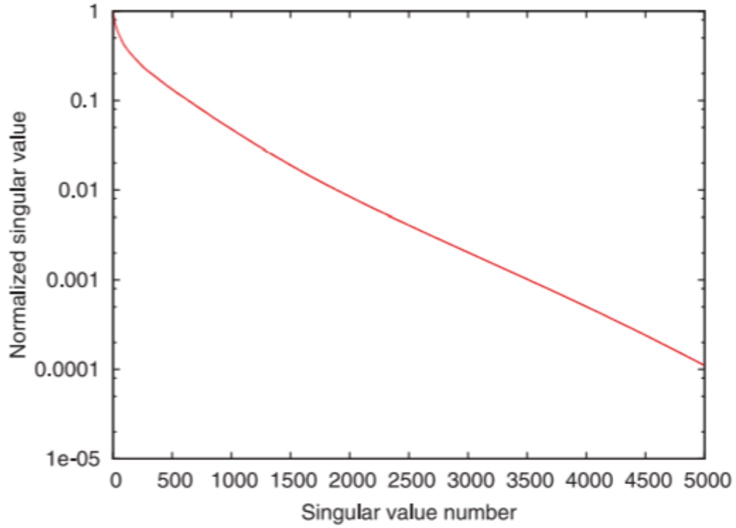

Normalized singular value
Singular value number
1
0.1
0.01
0.001
0.0001
1e-05
0
500
1000
1500
2000
2500
3000
3500
4000
4500
5000

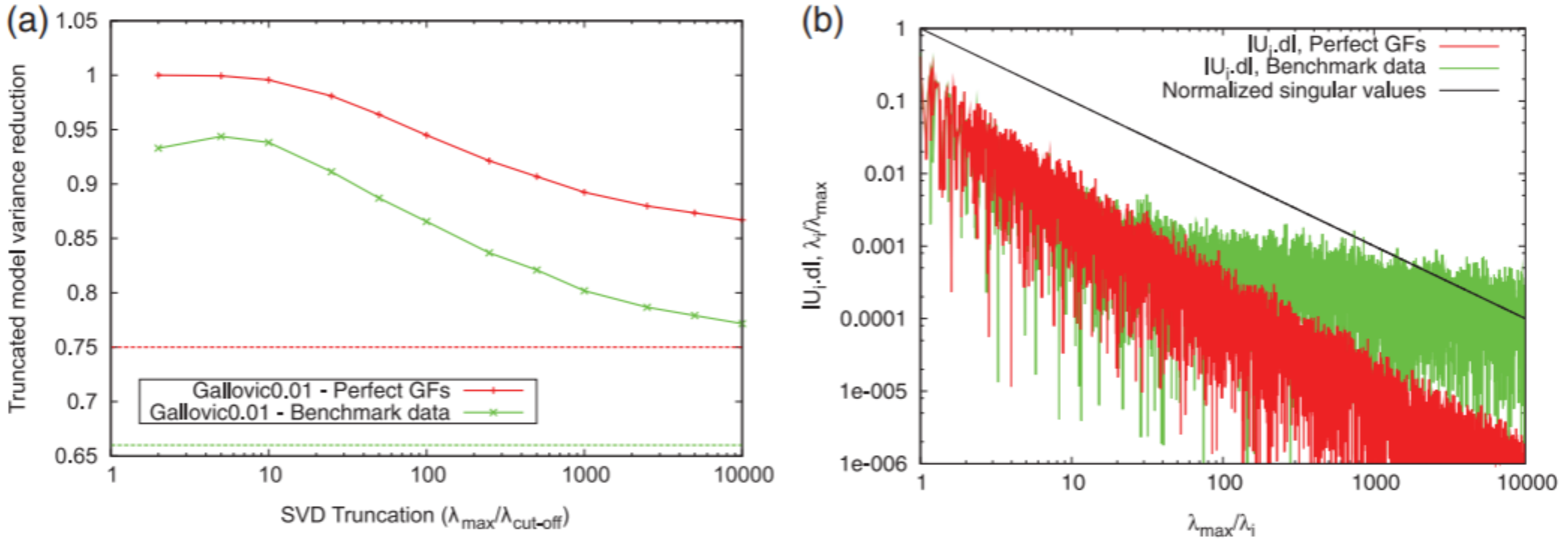

(a)
Truncated model variance reduction
SVD Truncation ($\lambda_{max}/\lambda_{cut\text{-}off}$)
Gallovic0.01 - Perfect GFs
Gallovic0.01 - Benchmark data
1.05
1
0.95
0.9
0.85
0.8
0.75
0.7
0.65
1
10
100
1000
10000
(b)
$|U_i.d|$, λ_i/λ_{max}
λ_{max}/λ_i
$|U_i.d|$, Perfect GFs
$|U_i.d|$, Benchmark data
Normalized singular values
1
0.1
0.01
0.001
0.0001
1e-005
1e-006
1
10
100
1000
10000

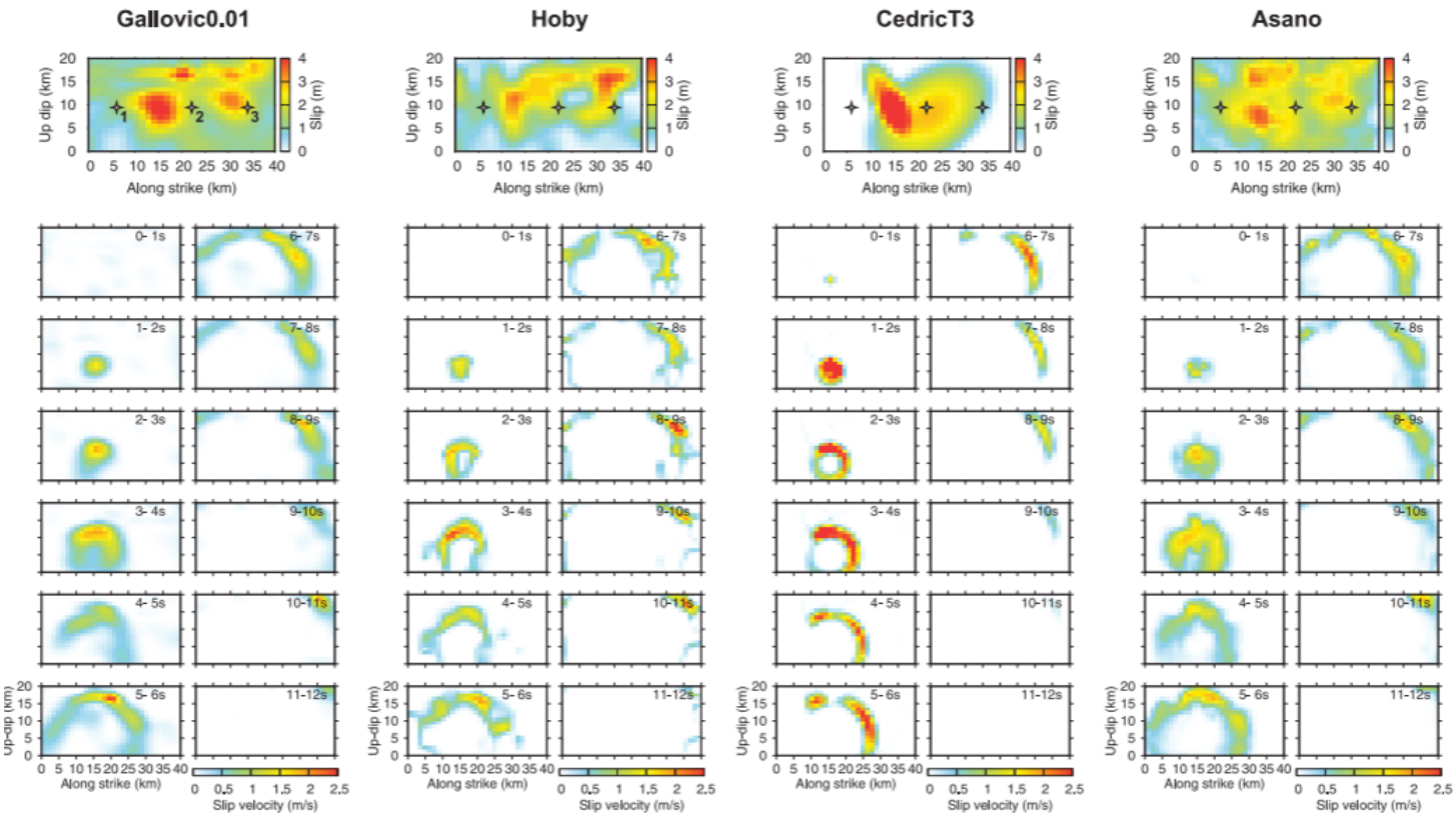

Gallovic0.01
Hoby
CedricT3
Asano
Up dip (km)
Along strike (km)
Slip (m)
0- 1s
1- 2s
2- 3s
3- 4s
4- 5s
5- 6s
6- 7s
7- 8s
8- 9s
9-10s
10-11s
11-12s
Up-dip (km)
Slip velocity (m/s)

Raw

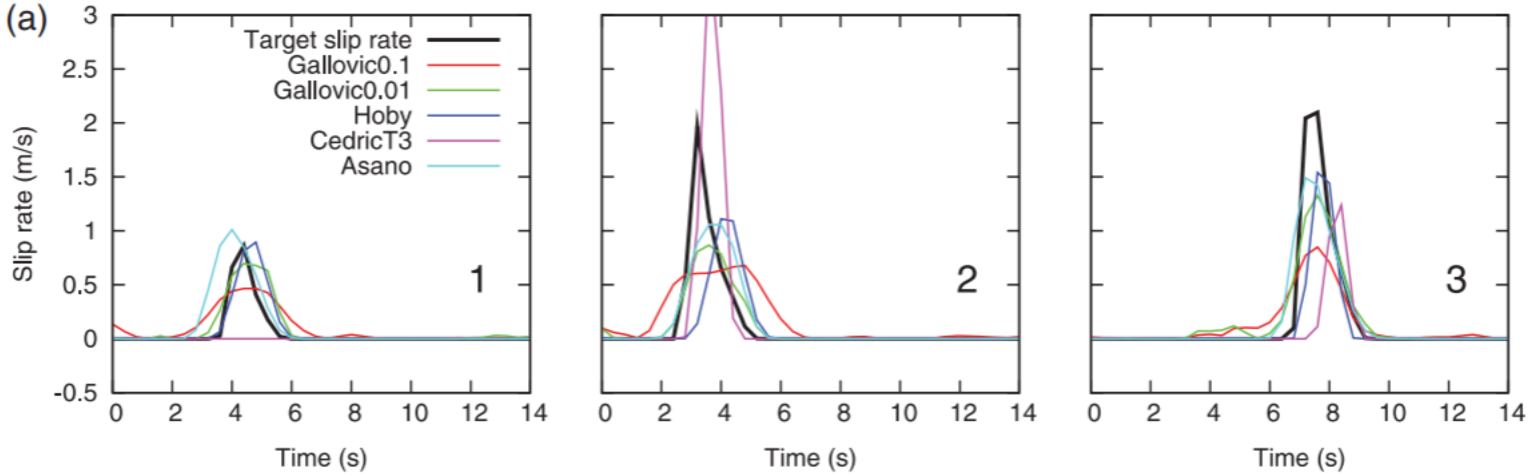

After truncation

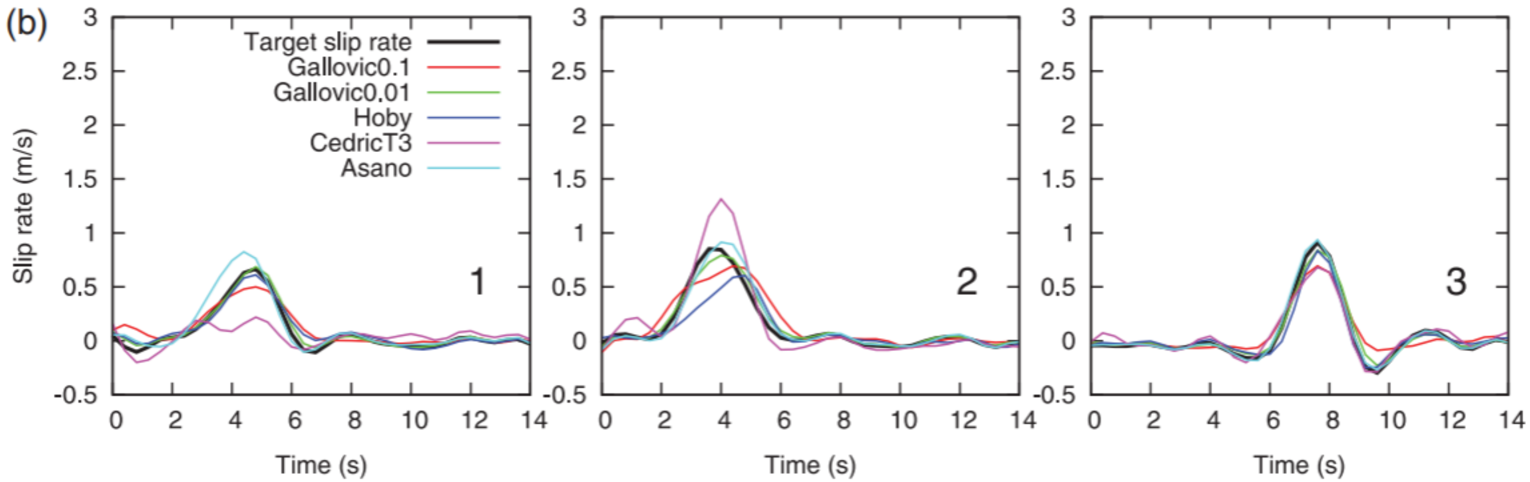

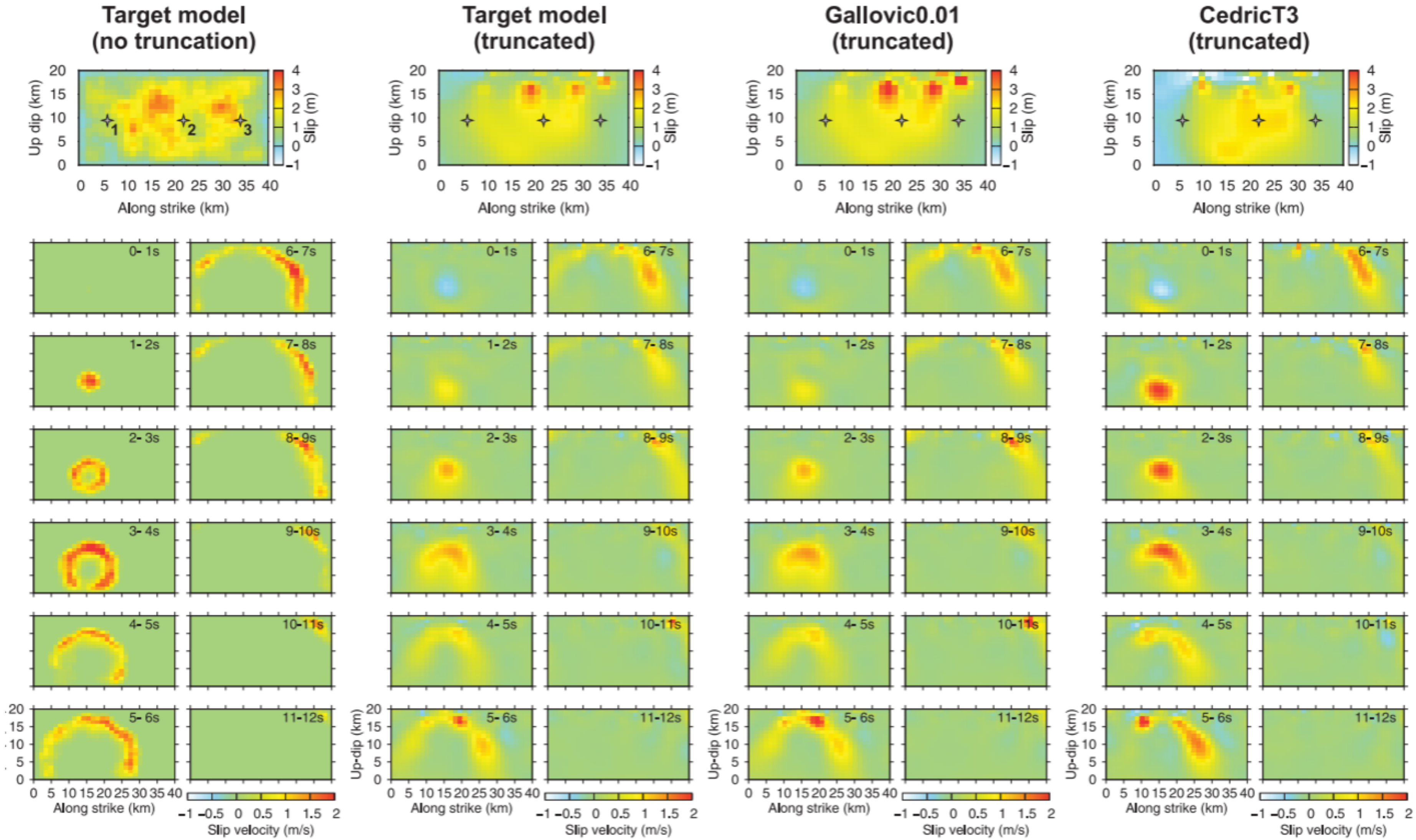
Target model
(no truncation)
Target model
(truncated)
Gallovic0.01
(truncated)
CedricT3
(truncated)
Up dip (km)
Along strike (km)
Slip (m)
Up-dip (km)
Slip velocity (m/s)
0- 1s
1- 2s
2- 3s
3- 4s
4- 5s
5- 6s
6- 7s
7- 8s
8- 9s
9-10s
10-11s
11-12s

Eigenvalues of $G^T G$

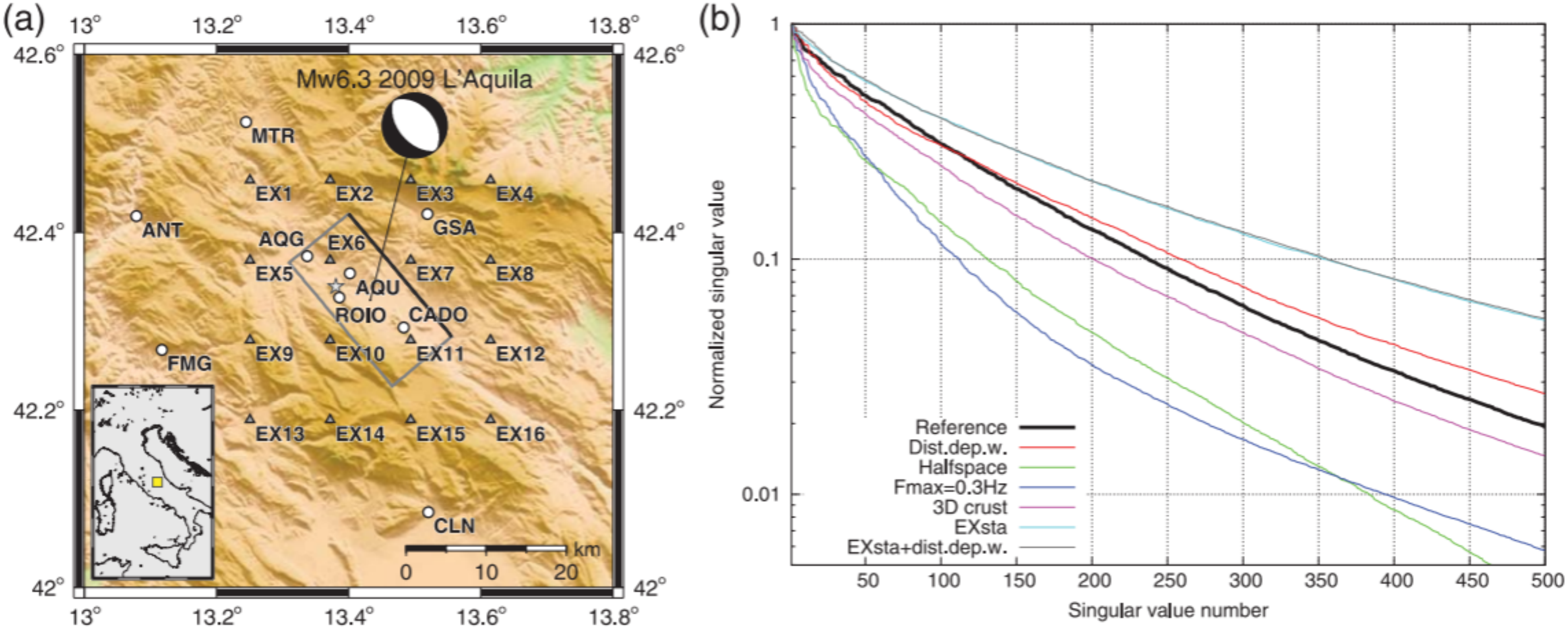

Eigenvalues of $G^T G$

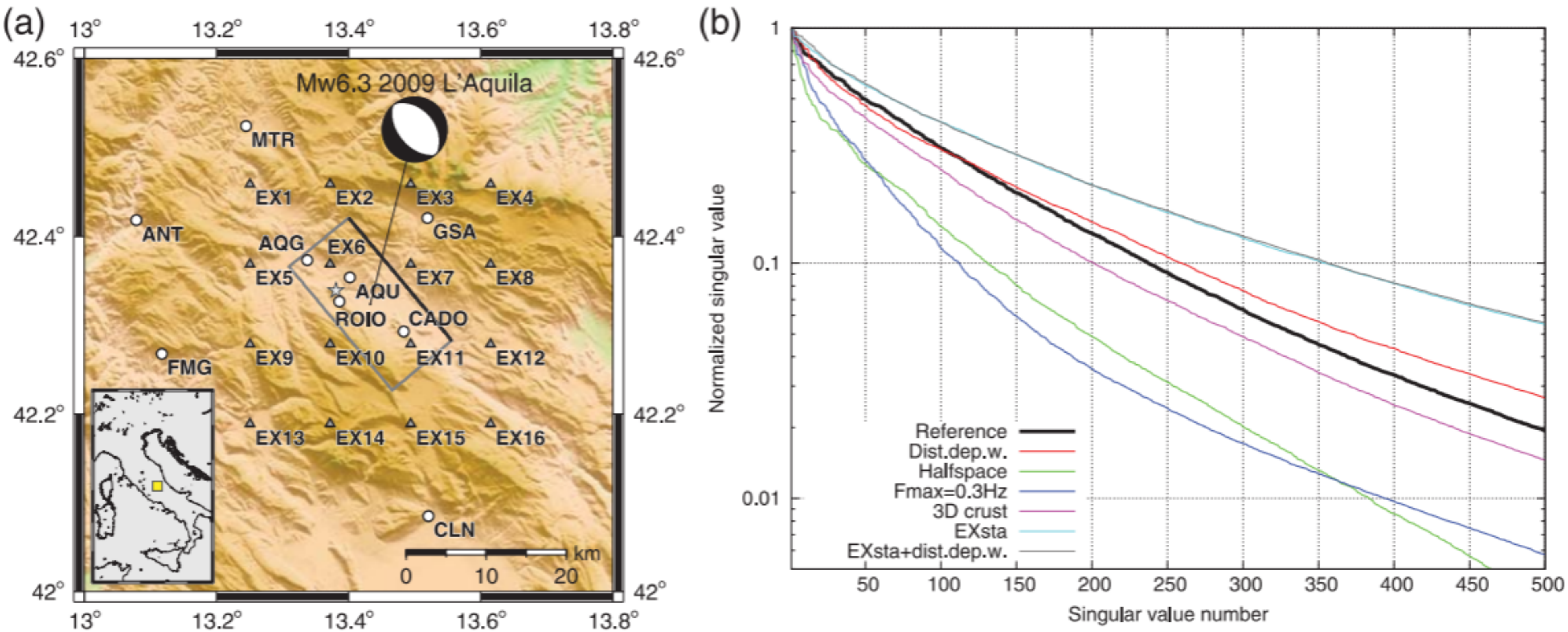

Dealing with an
ill-conditioned inverse problem

4 slip models of the 1992 Mw 7.3 Landers earthquake from SRCMOD

Minson et al (2013)

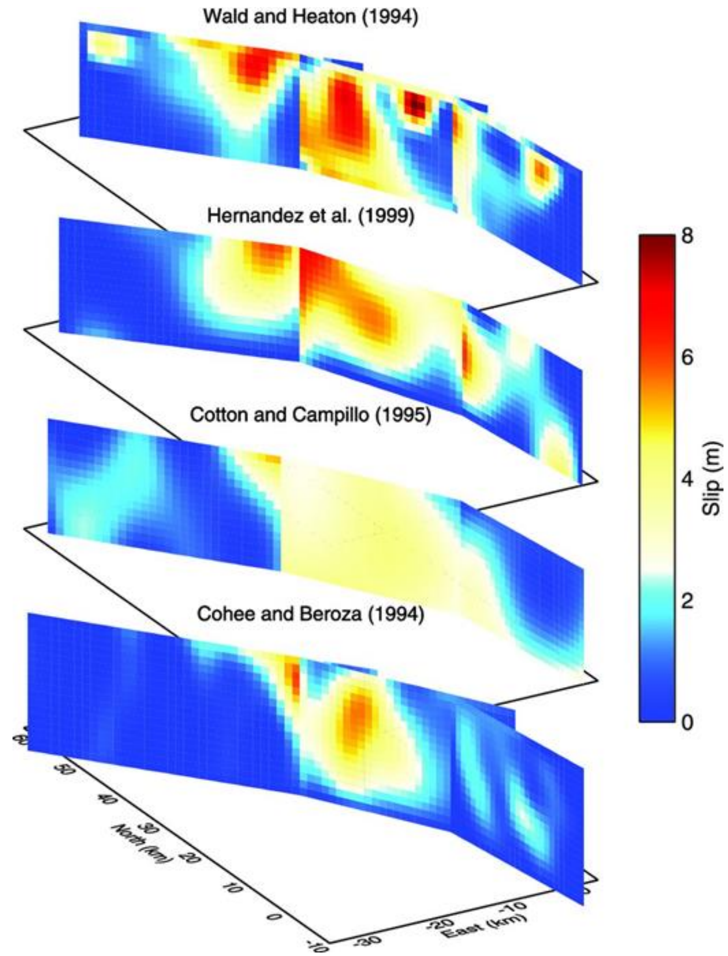

Regularization

Linear inverse problem: find m^* that minimizes the cost function

$$C(m) = \|d - G \cdot m\|^2$$

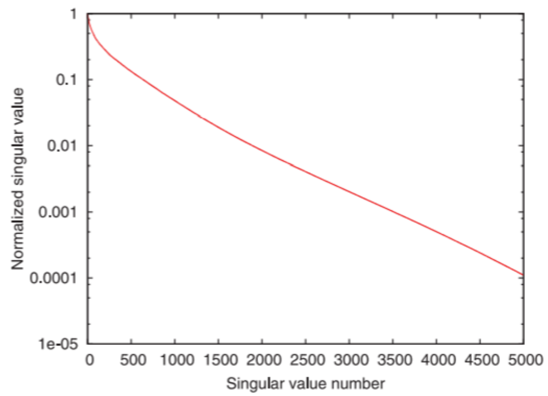

SVD components of data and model are related by

$$\tilde{m}_i = \tilde{d}_i / \lambda_i \qquad \text{where } \lambda_i \text{ are the eigenvalues of } G^T G$$

With data noise: $\tilde{m}_i = \tilde{d}_i / \lambda_i + \tilde{n}_i / \lambda_i$

Small λ_i → noise amplification, ill-conditioning

Tikhonov regularization:

$$C(m) = \|d - G \cdot m\|^2 + \epsilon \|m\|^2$$

$$\tilde{m}_i = \tilde{d}_i \, \lambda_i / (\lambda_i^2 + \epsilon)$$

For small eigenvalues $\lambda_i \ll \epsilon$: $\tilde{m}_i = \tilde{d}_i \lambda_i / \epsilon + \tilde{n}_i \lambda_i / \epsilon$

Limited effect of small eigenvalues → noise damped, better conditioning

Regularization

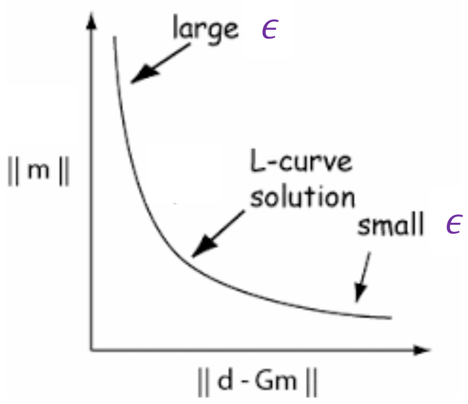

An ill-conditioned problem has a stable solution only if additional assumptions are made

Tikhonov regularization: Minimize $\|d - G \cdot m\|^2 + \epsilon\|m\|^2$

Equivalent formulation:

Minimize $\|d - G \cdot m\|^2$ subject to $\|m\| \leq \delta$

This is the additional assumption

There is a monotonic relation between the regularization parameters δ and ϵ.

More general Tikhonov regularization:

Minimize $\|d - G \cdot m\|^2 + \epsilon\|L \cdot m\|^2$ where L is often a gradient operator

→ assumption of model smoothness

Regularization

An ill-conditioned problem has a stable solution only if additional assumptions are made.

Typical assumptions:

- Smoothness (in time and/or space)
- Positivity (of slip velocity)
- Limited ranges (of rupture speed, rupture area, rake)
- Prescribed slip rate function shape
- Combine multiple data types

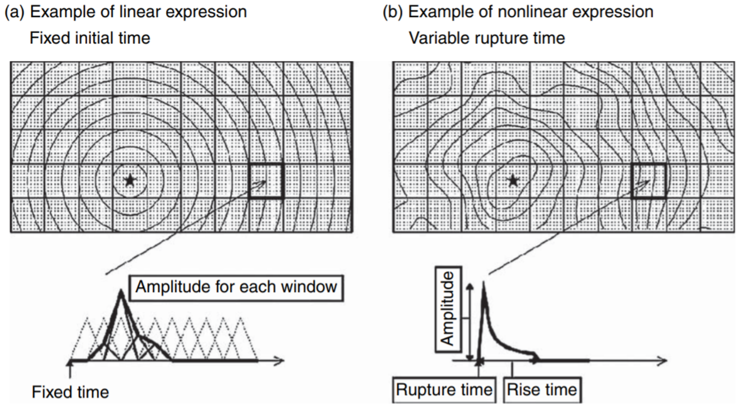

Some assumptions break the linearity of the inverse problem.

Some assumptions restrict strongly the type of ruptures allowed (e.g. single rupture front).

Back-propagating rupture pulses

Assumptions made to regularize the inverse problem may restrict the type of ruptures allowed, e.g. single rupture front.

→ Limits on discovery of complex rupture patterns, e.g. multiple rupture fronts.

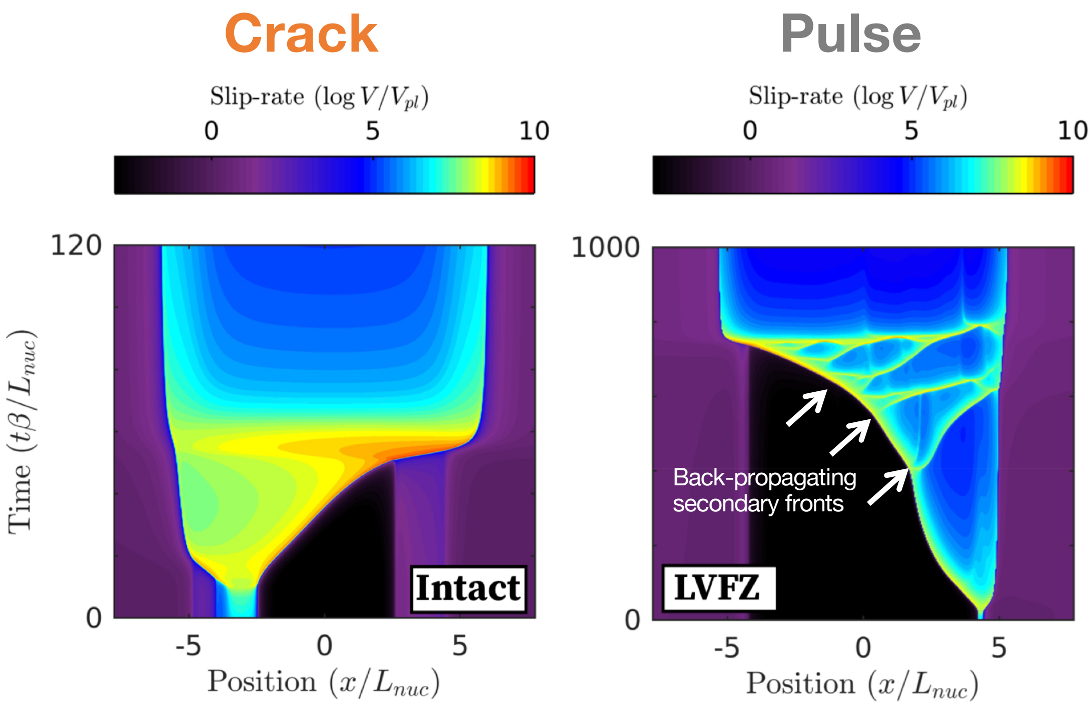

Bayesian inversion

Bayes' theorem, probabilities relating data and model:

$$p(m|d) \propto p(d|m)\, p(m)$$

Posterior

Prior

Prob. of having observed d, given m

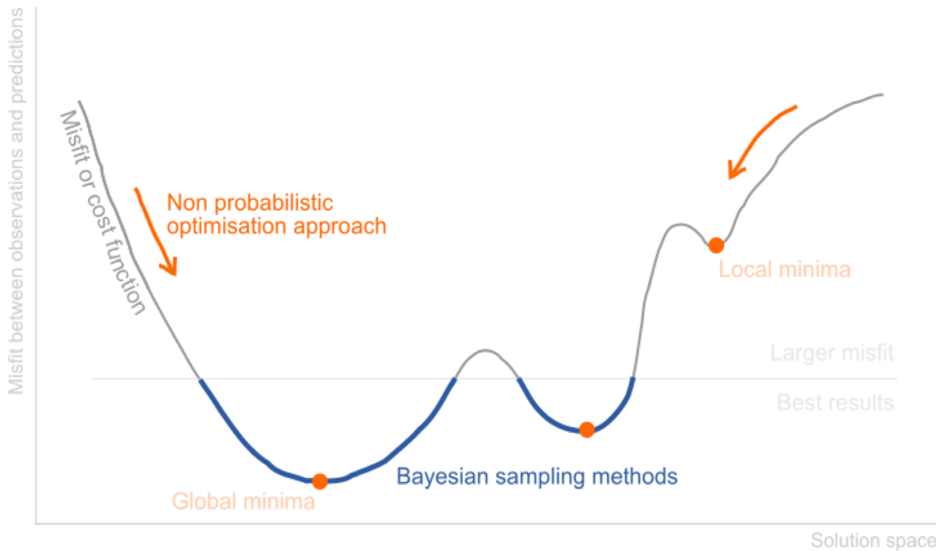

T. Ragon

Bayesian inversion: sampling the posterior probability
Result = a family of models and their likelihood

Bayesian inversion

Bayes' theorem, probabilities relating data and model:

$$p(m|d) \propto p(d|m)\, p(m)$$

Posterior

Prior

Prob. of having observed d, given m

Bayesian inversion: sampling the posterior probability
Result = a family of models and their likelihood

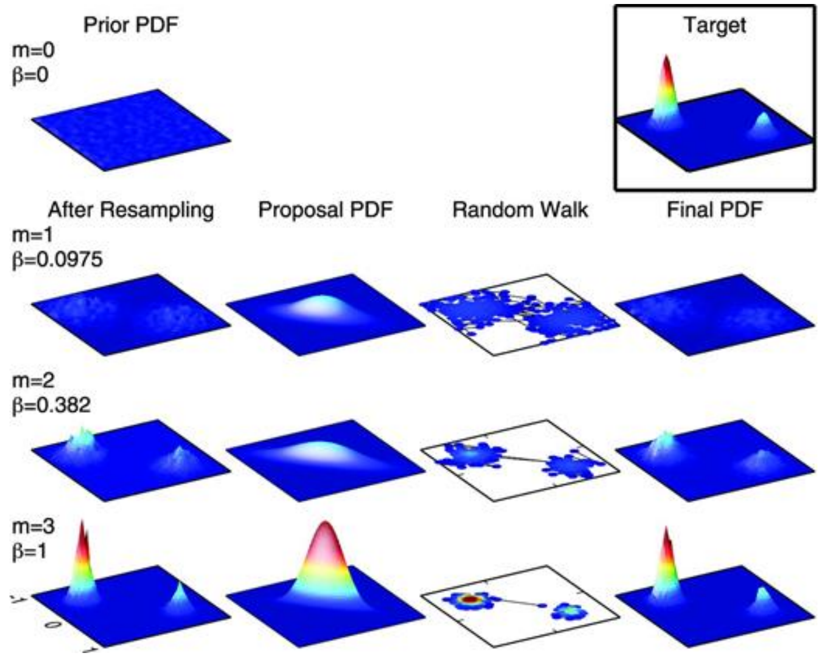

CATMIP algorithm by Minson et al (2013)

Bayesian inversion

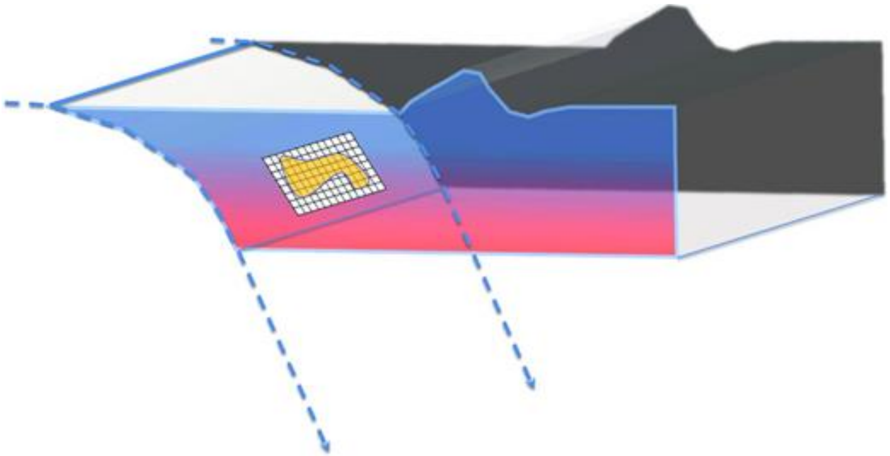

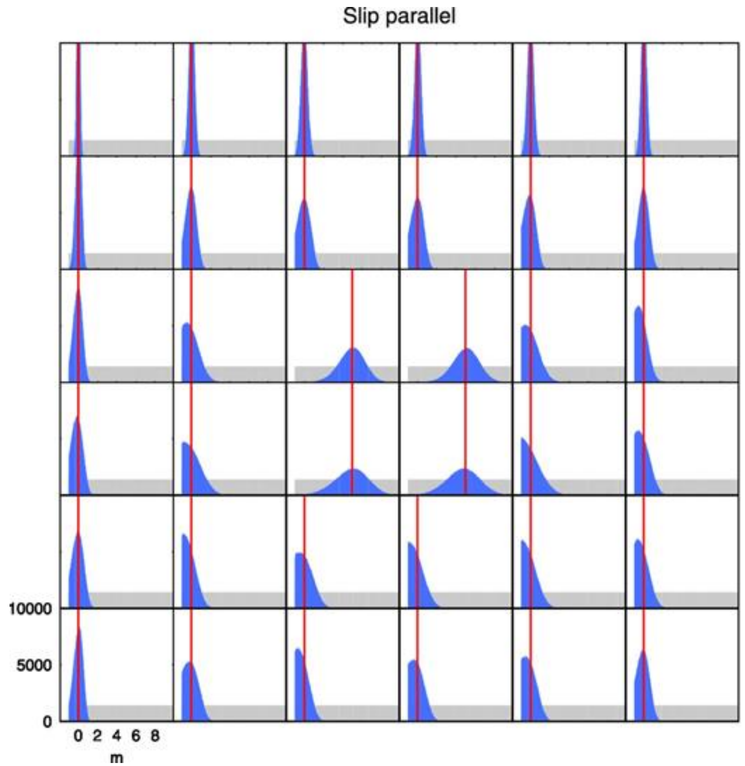

Prior
Posterior
True

Minson et al (2013)

Bayesian inversion

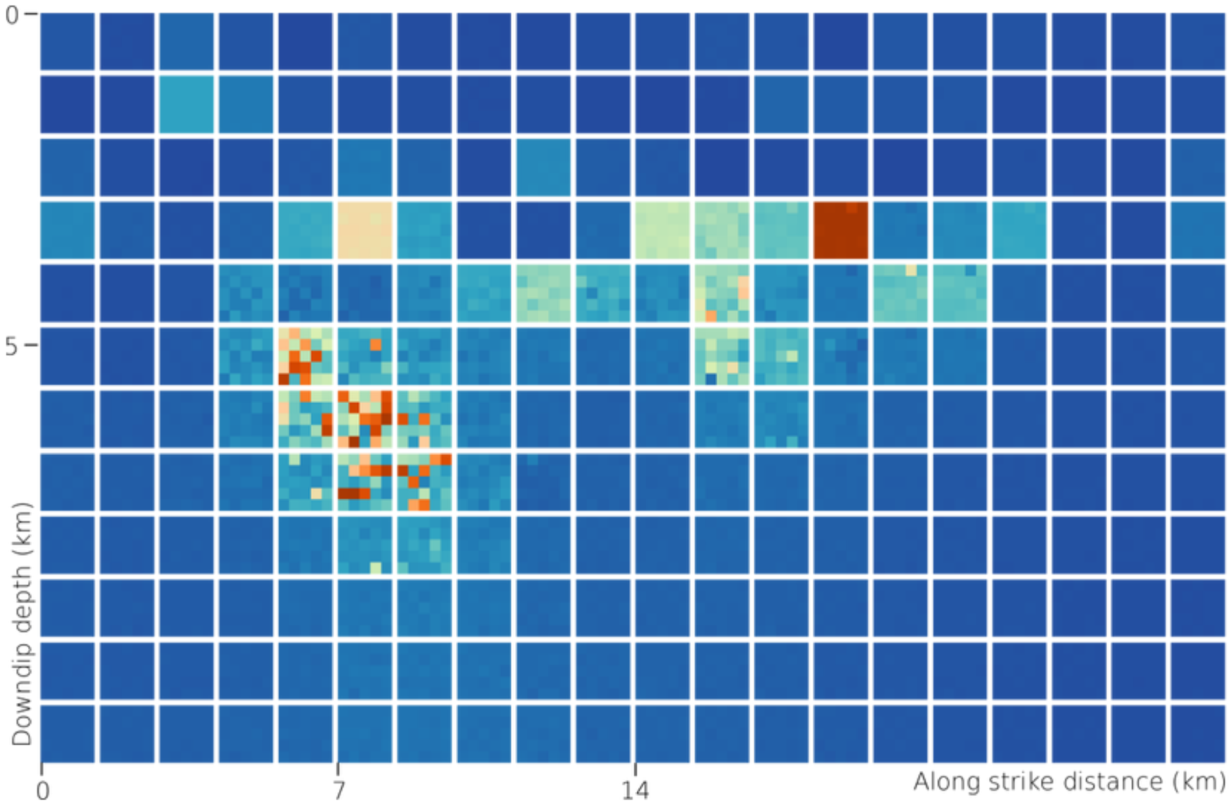

Co-seismic slip of the 2016 Amatrice earthquake Mw6.2.

The median value of each family of models is shown in each sub-pixel.

T. Ragon

Bayesian inversion

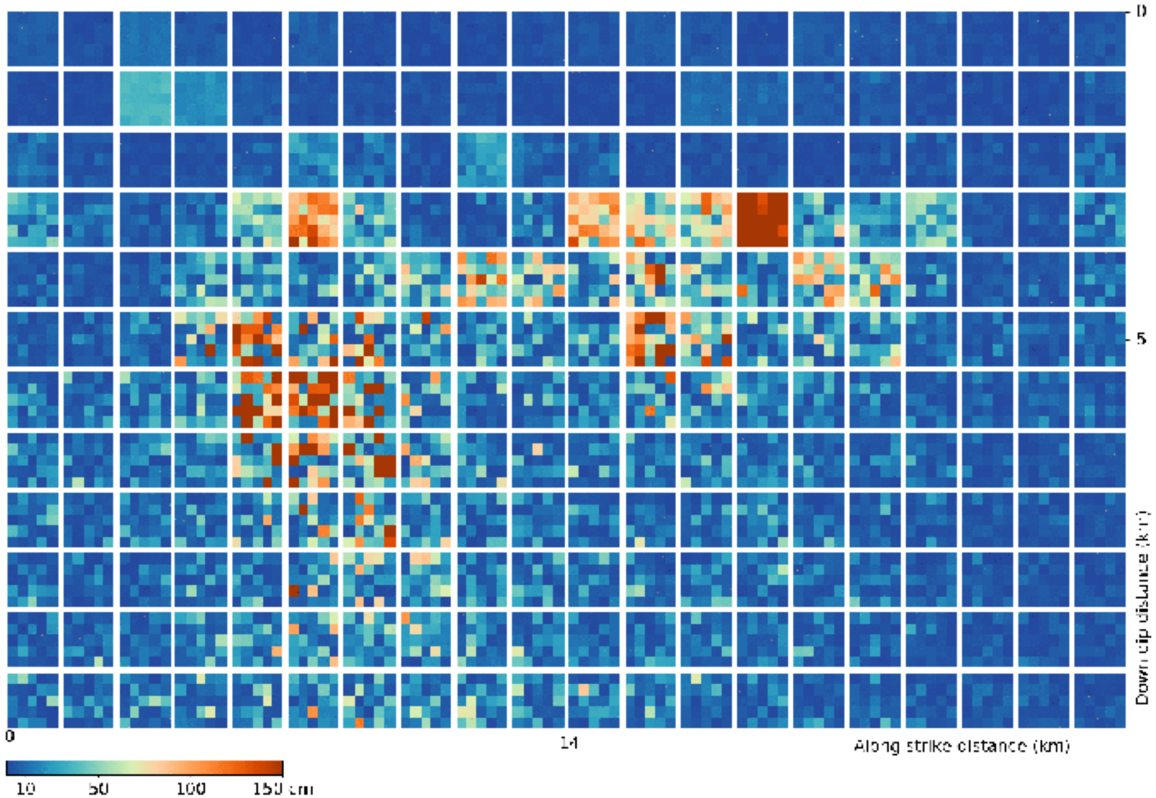

Animated co-seismic slip of the 2016 Amatrice earthquake, Mw6.2.

Random samples are shown in each family of models.

T. Ragon

Example: 2014 Mw 8.1 Iquique earthquake

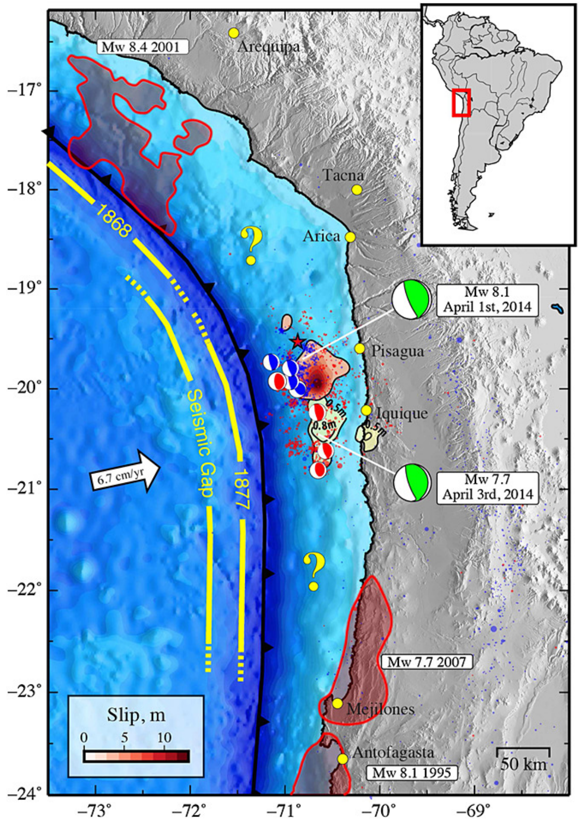

Multiple data types:

- Static: GPS, InSAR, tsunami
- Kinematic: : seismograms, cGPS

Model parameters:

- Static m_s: final slip
- Kinematic m_k: rupture speed, rise time

Two-step approach:

1. Static: $p(m_s|d_s) \propto p(d_s|m_s)\, p(m_s)$

2. Kinematic:

$$p(m_k, m_s|d_k, d_s) \propto p(d_k|m_k, m_s)\, p(m_s|d_s) p(m_k)$$

Duputel et al (GRL 2015)

Example: 2014 Mw 8.1 Iquique earthquake

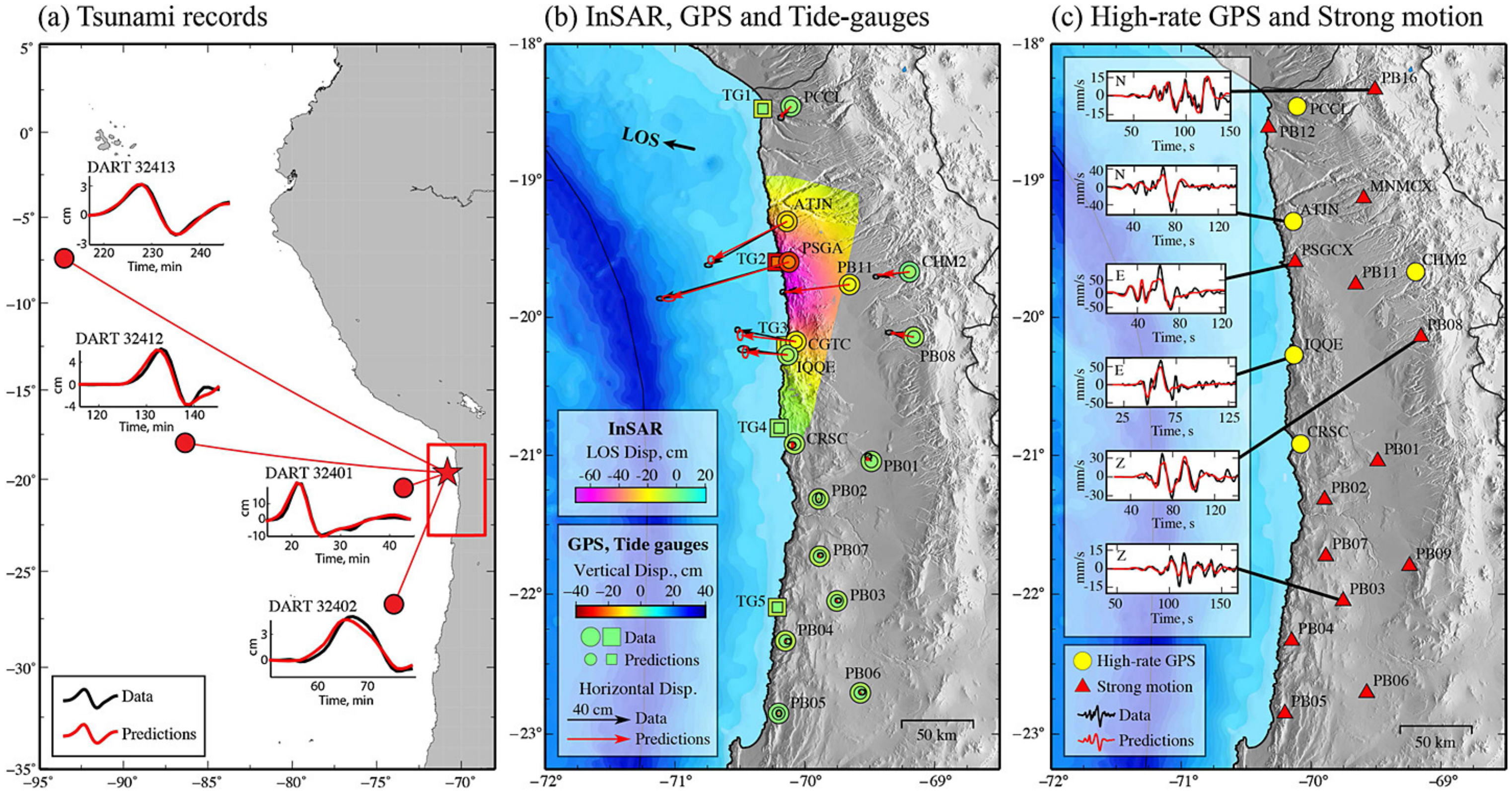

Duputel et al (GRL 2015)

Example: 2014 Mw 8.1 Iquique earthquake

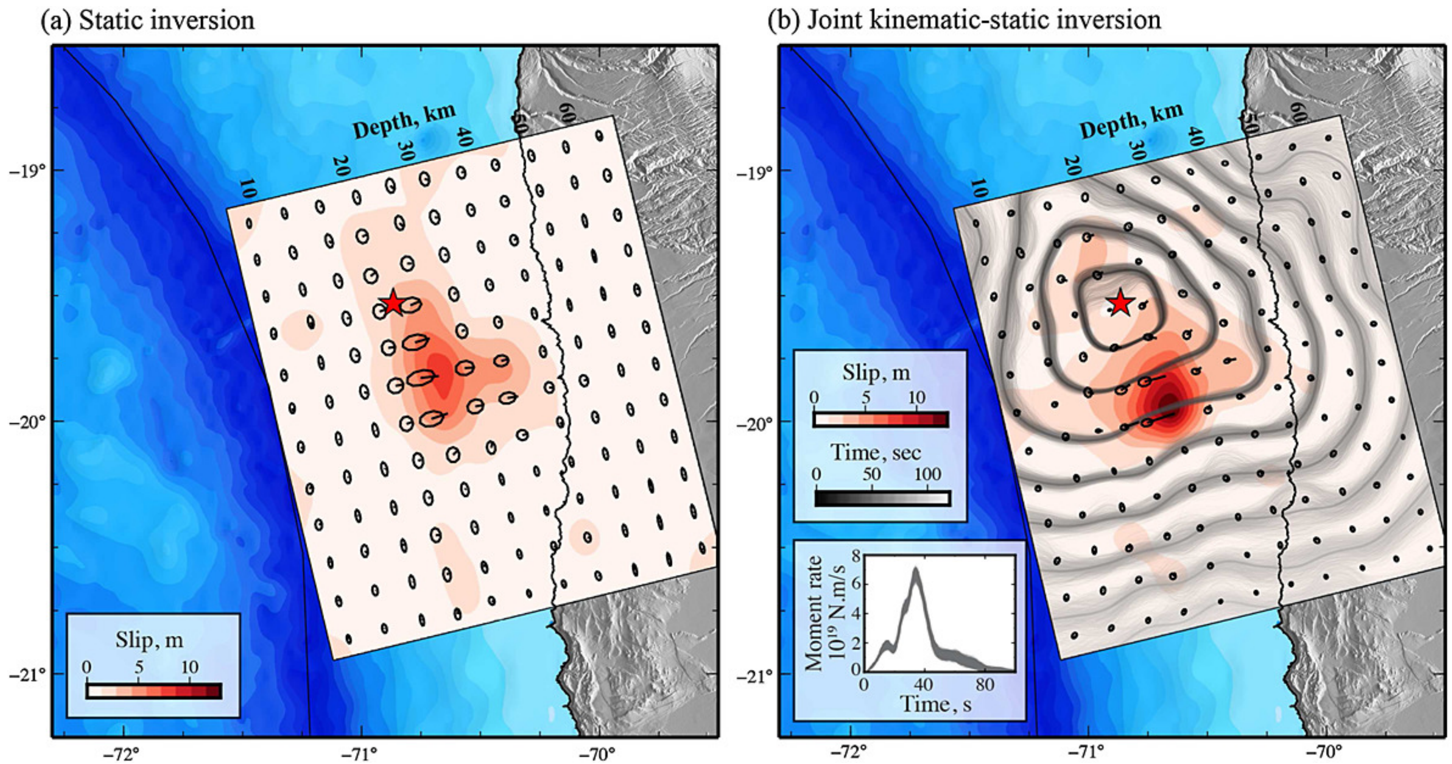

Duputel et al (GRL 2015)

Example: 2014 Mw 8.1 Iquique earthquake

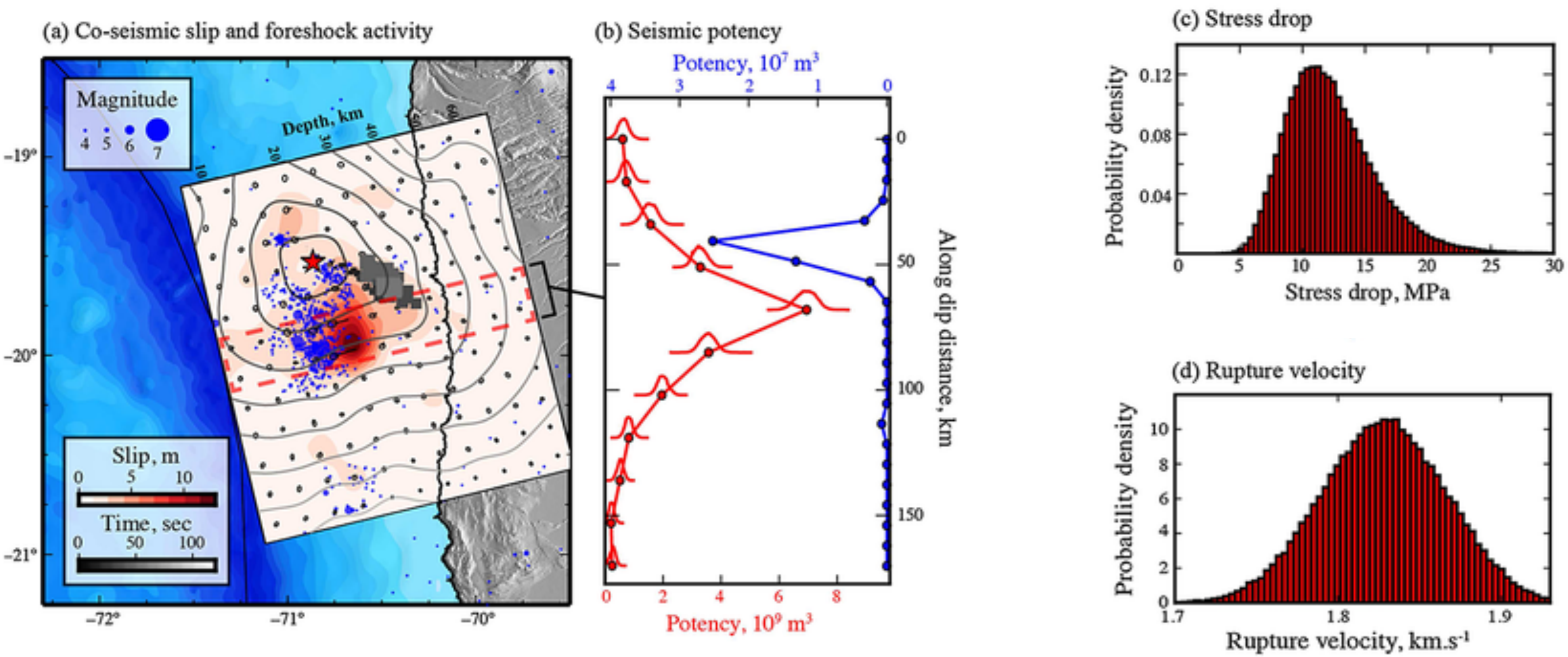

Duputel et al (GRL 2015)

Fig S2 of Duputel et al (comparison to other inversions)
Fig S13 (sensitivity)

Dealing with
uncertainties of the forward-modeling

Uncertainties in G

Linear forward problem:

Given m, compute $d = G \cdot m$

Linear inverse problem:

Given d, find m that minimizes $\|d - G \cdot m\|^2$

But G is not perfect:

- Uncertainties in the Earth's velocity model
- Uncertainties in fault geometry
- Approximations and inaccuracies in the computation of G

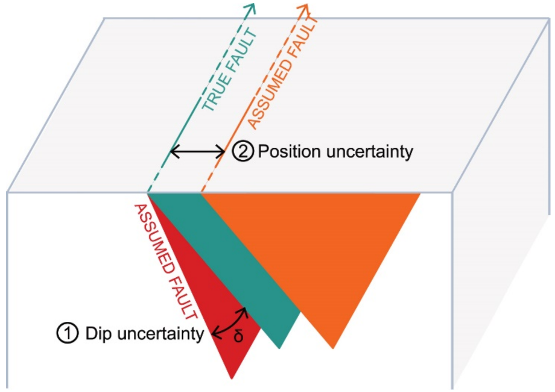

Uncertainties in G

Cost function of inverse problem

$$\|d - G \cdot m\|^2 = (d - G \cdot m)^T (d - G \cdot m)$$

Including data covariance matrix C_d :

$$(d - G \cdot m)^T C_d^{-1} (d - G \cdot m)$$

Assume $G = G(\Psi)$ where Ψ are parameters of fault geometry, crustal wave speeds, etc.
with covariance matrix C_Ψ.
Accounting for modelling uncertainties:

$$(d - G \cdot m)^T C^{-1} (d - G \cdot m)$$

where

$$C = C_d + \boldsymbol{C_p(m)}$$

$$C_p = K \cdot C_\Psi \cdot K^T$$

$$K_{ijk} = \frac{\partial G_{ij}}{\partial \Psi_k} \left(\Psi_{prior}\right)$$

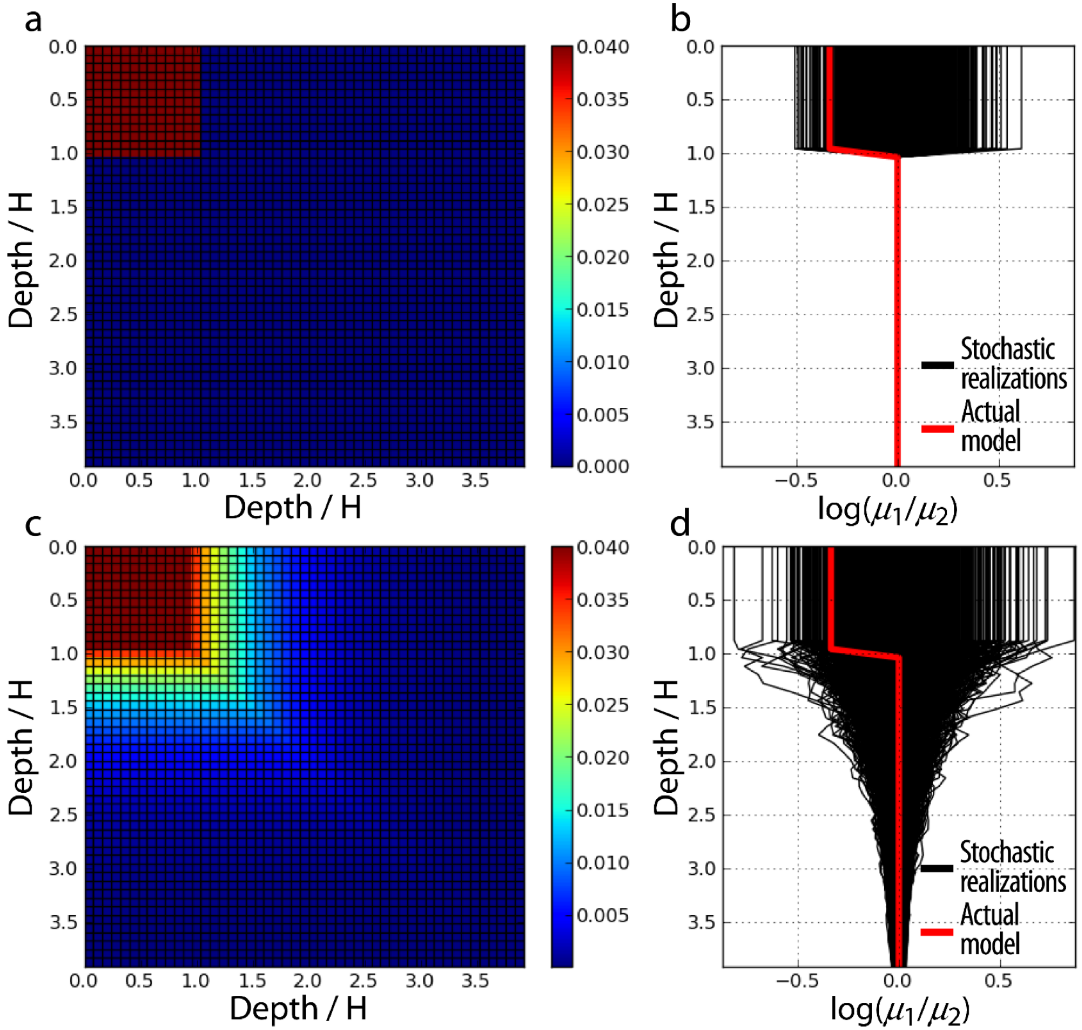

Duputel et al
(2014)

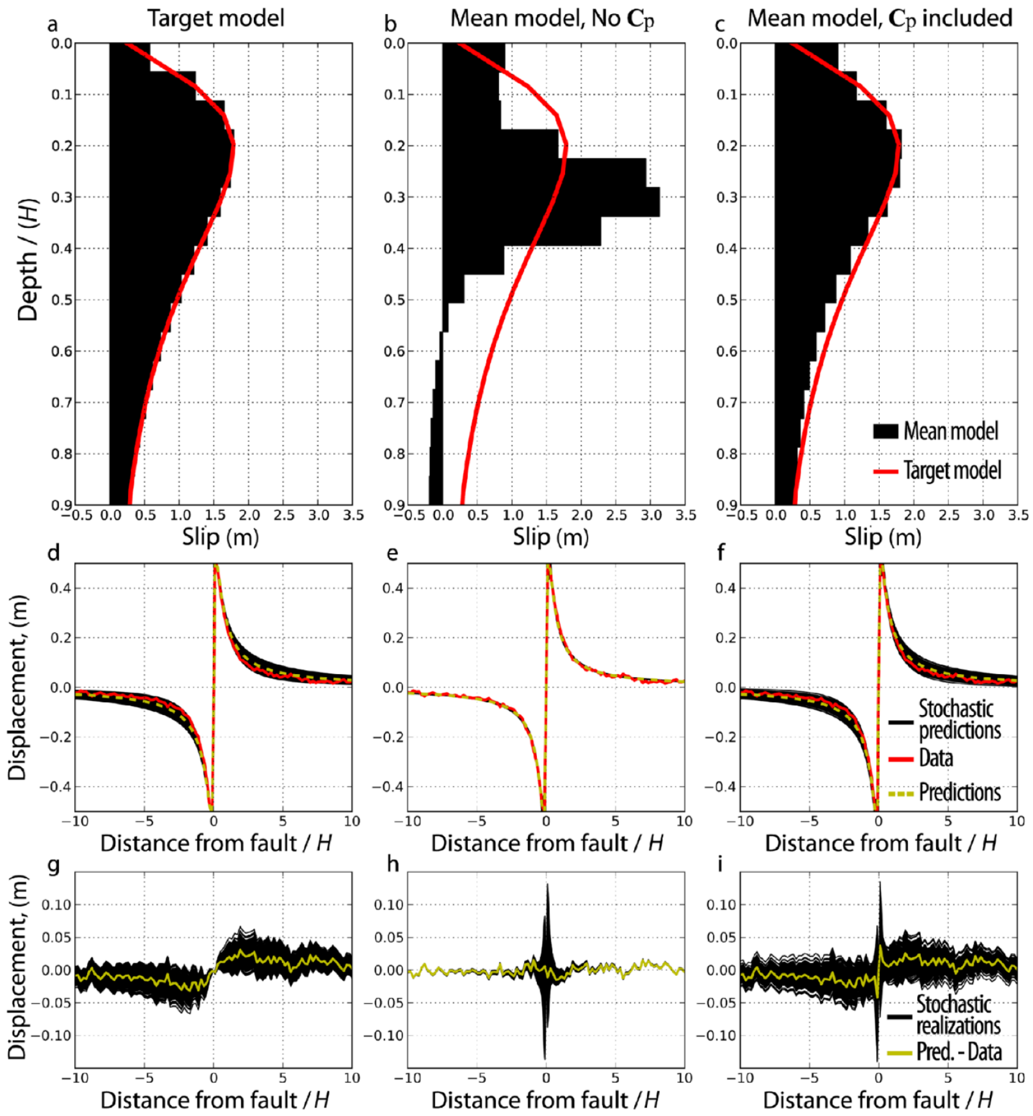

Duputel et al
(2014)

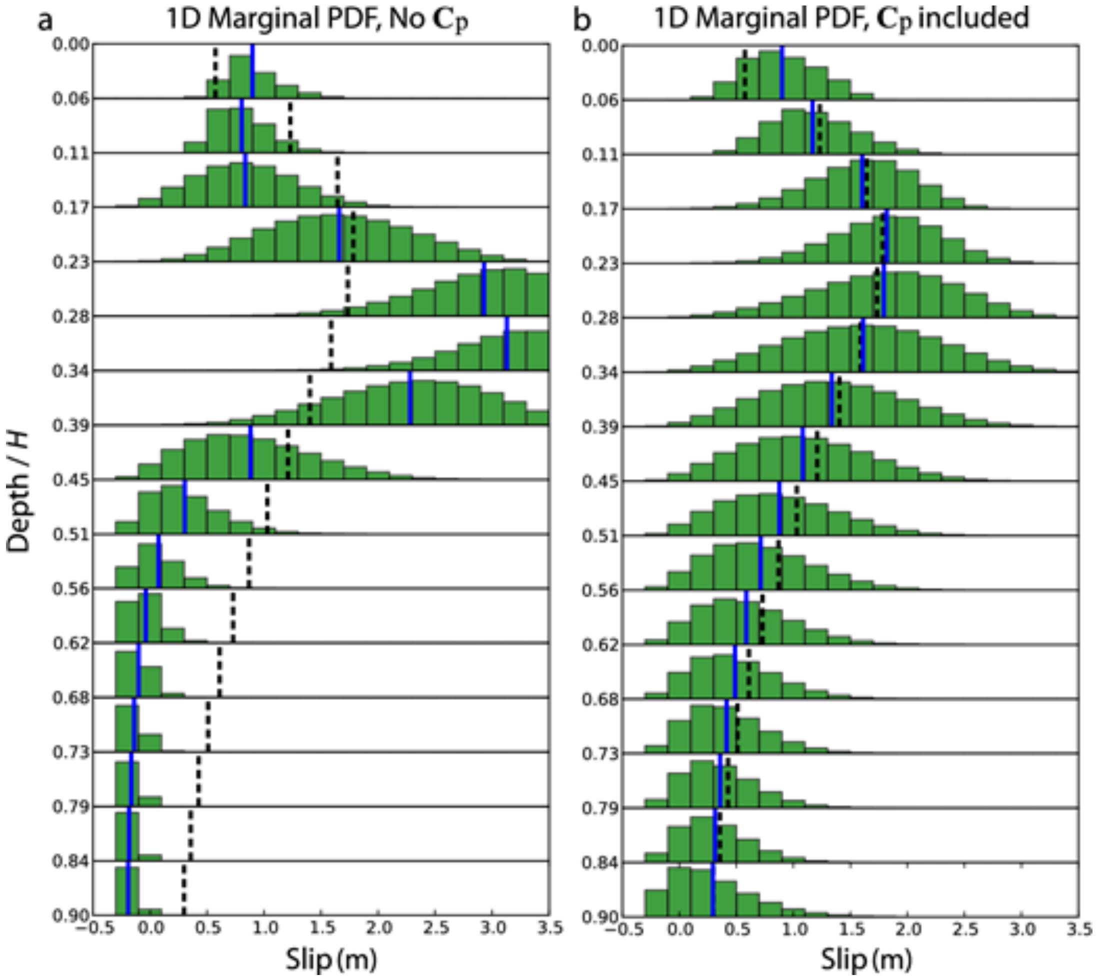

Duputel et al
(2014)

Fig S6 of Duputel et al Iquique

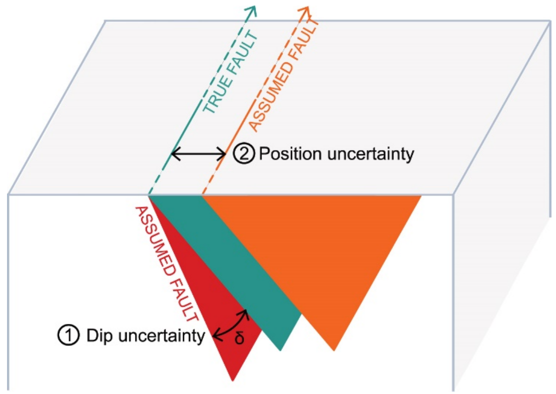

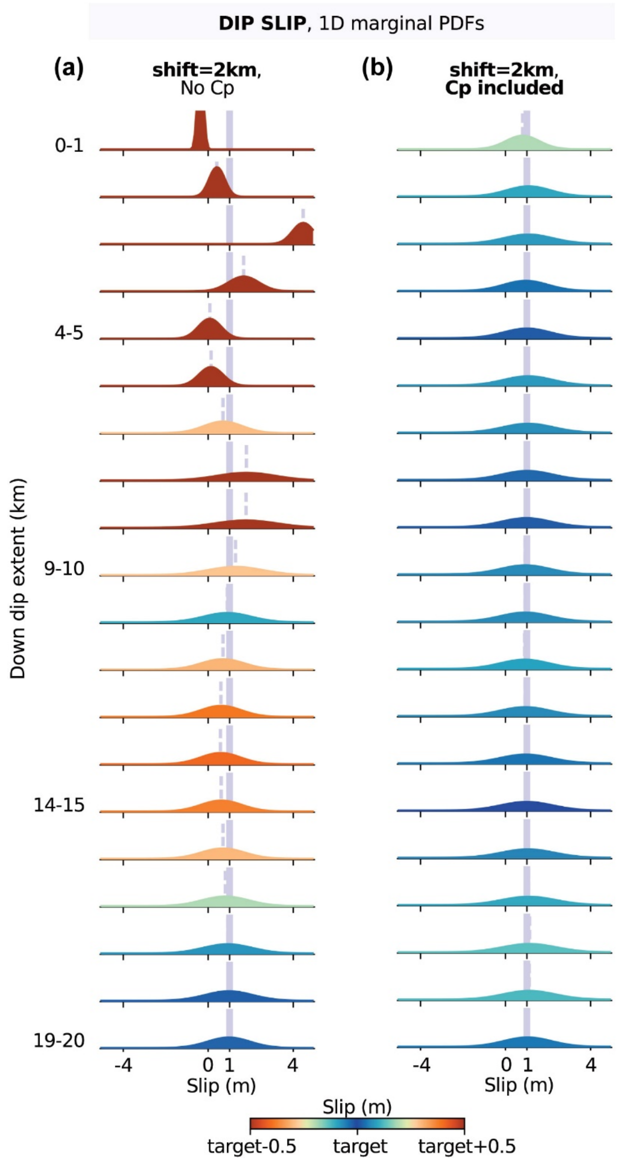

Ragon et al (2018)